Interaction Notes

Note 588

December 13, 2003
Revised June 8, 2004

On the Addition of EM Field Propagation and Coupling Effects in the BLT Equation

F.M. Tesche
C. M. Butler

Holcombe Dept. of Electrical and Computer Engin.
College of Engineering & Science
337 Fluor Daniel Building
Box 340915
Clemson, SC 29634-0915

Abstract

This note discusses the extension of the Baum-Liu-Tesche (BLT) equation to include the effects of propagating EM fields and their coupling to transmission line structures. The usual BLT equation describes the propagation of voltage (and current) waves along transmission lines. In the extended BLT formalism, both voltage and E-field quantities are treated together and this permits the addition of scatterers and apertures in the models.

Work conducted under the provisions of AFOSR MURI Grant F49620-01-1-0436

Contents

Figures

On the Addition of EM Field Propagation and Coupling Effects in the BLT Equation

1. Introduction

Recent developments in electromagnetic (EM) field sources producing high power microwave (HPM) or ultra wide-band (UWB) transient signals have led to a concern about the effects of these environments on modern digital systems. Such excitations, which collectively are referred to as high power electromagnetic (HPEM) fields, could be inadvertent, like the environment produced by a search radar illuminating a nearby aircraft, or intentional, such as a deliberate attack on a system by an adversary using an electromagnetic weapon [1]. In either case, the effects of these HPEM fields may include system upset, and in some cases, permanent damage.

Figure 1 illustrates a simple example of an electrical system excited by an external HPEM source. This energy source can provide either a narrow-band pulsed EM field, or a fast transient field that couples energy onto the long lines attached to the system. Additionally, the incident field excites various apertures of the system enclosure. This EM energy is able to penetrate into the system, is distributed within the internal circuitry, and ultimately arrives at the digital components, at which point an upset or failure may occur. Of course, if the system is well shielded, the internal components may not be affected by this excitation; however all systems must have imperfections in the external shielding (for access hatches, power penetrations, etc.) and the survival of such a system is never 100% assured.

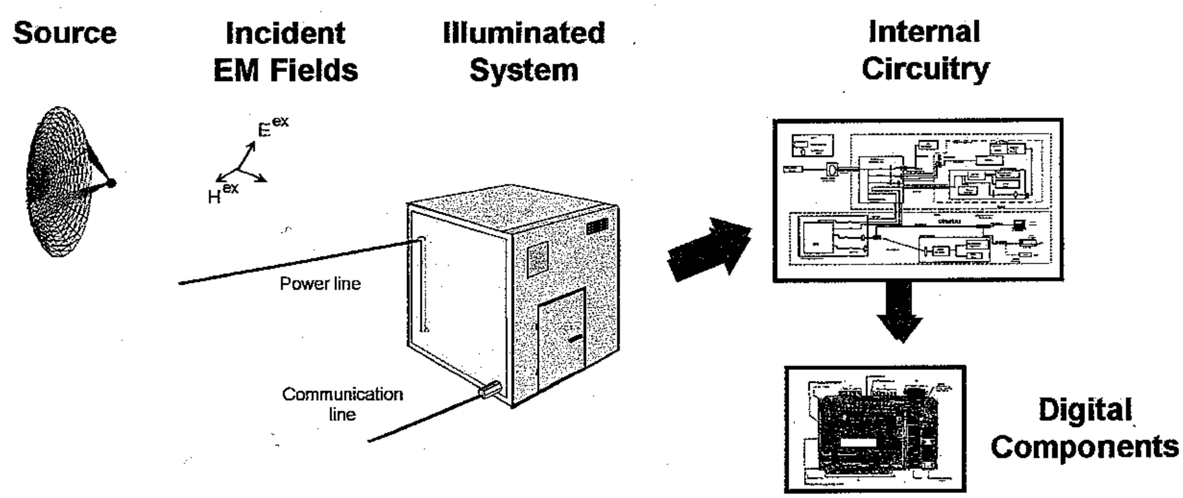

Figure 1. Illustration of an electrical system excited by an external EM source, causing upset or damage in the internal circuitry.

To better understand the possible effects of the HPEM environments on such electrical systems, it is desired to develop a computational modeling approach that will allow an analyst to estimate the transient responses at the component level – both in amplitude and wave form – and to conduct trade studies to examine the effectiveness of various system design changes or shielding configurations. The purpose of this report, therefore, is to outline a modeling approach that can be used for this purpose.

The HPEM problem posed in Figure 1 is similar to past problems involving the protection of electronic equipment against the effects of the nuclear electromagnetic pulse (NEMP) [2]. Although the NEMP threat is lower in frequency (with a spectral content from several kHz to about 100 MHz), there is a common point of departure for the analysis that can be used in the present case. In the NEMP analysis, the modeling of electromagnetic (EM) field interaction with a complex system or facility has been accomplished by the introduction of the concept of electromagnetic topology. This idea was initially developed by Baum [3], and later formalized in the literature [4, 5, 6, 7]. This methodology permits the system to be viewed as a collection of conducting surfaces that attenuate the incident EM field environment and effectively shield the interior regions from the external field.

For the sample system of Figure 1, the topological representation of the shielding surfaces is shown in Figure 2. These shielding surfaces are not perfect, however, as there may be conductors passing through the surfaces, and external EM energy can penetrate into the system via current and charge flowing on the conductors. Moreover, there may be apertures (holes) in the shielding and EM fields may penetrate into the interior. Finally, EM field diffusion through the shield material is a possibility, if the shield material is not highly conducting.

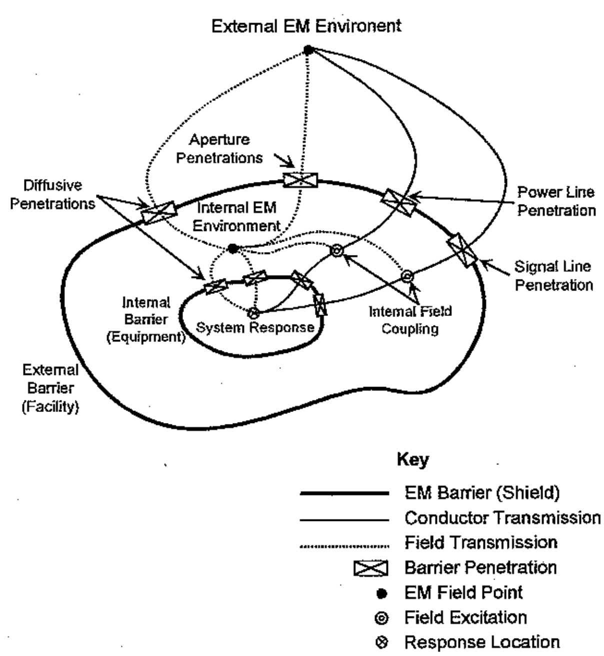

Figure 2. The system shielding topology diagram, showing the EM field interaction paths for the example facility of Figure 1.

To develop a computational model for the EM responses within the system, the concept of the interaction sequence diagram can be introduced. This is a diagram containing the main pathways that the EM energy takes as it penetrates into the system. Realizing that the most important paths are usually the "hard-wired", or conductive, paths[1], a considerable amount of work has been conducted on developing a way of computing the behavior of current and charge on interconnected wire networks. As an example, Figure 3 illustrates the conducting penetration paths within the interaction diagram of Figure 2, and it are these paths that the flow of EM energy must be modeled.

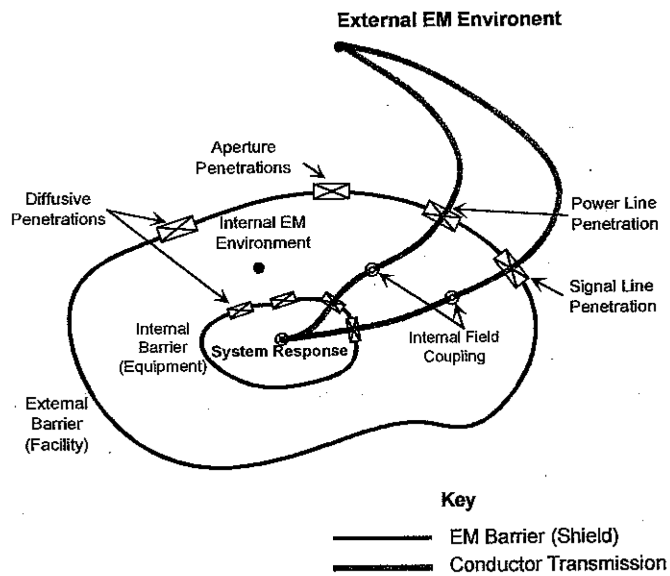

Figure 3. Simplified EM interaction paths for the sample system, as obtained by considering only the conducting penetration paths.

By using transmission line concepts, which result from a simplification of a complete solution of Maxwell's equations [8], a computationally simple model that predicts the propagation of EM energy into the system has been developed. This model is based on the Baum-Liu-Tesche (BLT) equation, which is a matrix equation describing the behavior of the voltage and/or current at all of the junctions (or interconnections) of the conductors in the network [6, 9, 10, 11]. In a sense, this equation is similar to a node analysis performed in conventional circuit theory, except that in the BLT equation, the effects of EM propagation along the individual conductors are considered.

Figure 4 shows a simple example of a network of interconnected transmission lines that can be analyzed by the BLT equation. In this case, each conductor is located over the reference

---

[1] For the case of NEMP modeling, the effects of the EM field coupling paths in the interaction sequence diagram are often neglected. This results in considerations of EM energy flow only along the conductors (e.g., the hard-wired lines). For the higher frequency HPEM analysis, the field coupling paths may be more important, and hence, they must be included in a more general model.

ground plane and at each open end of the line a terminating impedance is found. This network appears as if it were constructed by single-wire lines, but in reality, each transmission line can be a multiconductor bundle (a "tube") of conductors with the terminating impedances being generalized N-port loads. This diagram illustrates the network as having a simple tree-like configuration, although with the BLT analysis formalism, it is also possible to consider networks having one or more loops being formed by the transmission line tubes. Details of this type of analysis are provided in ref.[9].

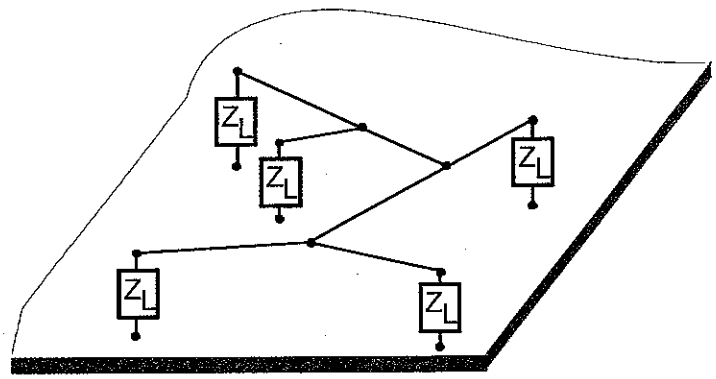

Figure 4. Example of a transmission line network, which is based on the simplification of the interaction sequence diagram.

Based on the topological modeling and the BLT equation, a computer code was written for analyzing transmission line networks like that of Figure 4. This early code was QV7TA and its operation is described in ref.[12]. Subsequent code development in France resulted in another code – CRIPTE – which is presently a commercially available code for performing a wide-band transmission line analysis. The details of this code and typical results have been described by Parmantier [13].

Figure 5 illustrates an example of the types of problems that can be analyzed using this modeling technique. Part *a* of the figure shows a cable harness located within the Electromagnetic Pulse Test Bed Aircraft (EMPTAC), which is a Boeing 707 aircraft that has been converted into a laboratory to validate EMP hardening technologies. This aircraft is located at the Kirtland AFB in Albuquerque, NM.

As a result of a collaboration between the Office National d'Etudes et de Recherches Aerospatiales (ONERA) (which is the is the French equivalent of NASA), the Centre d'Etudes de Gramat (CEG) and the Phillips Laboratory of the US Air Force, a combined analysis and measurement program was conducted to examine the accuracy of the CRIPTE code. Figure 5b illustrates the network model developed for this cable harness, and a comparison of the measured and computed results for voltages at one load in the network are shown in part *c*. As can be noted, the agreement between the model and measurements is quite good.

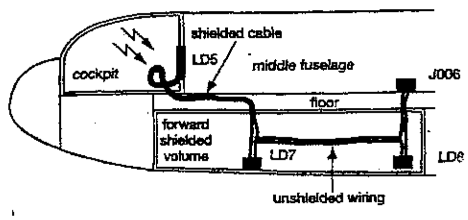

a. Cable harness within an aircraft system.

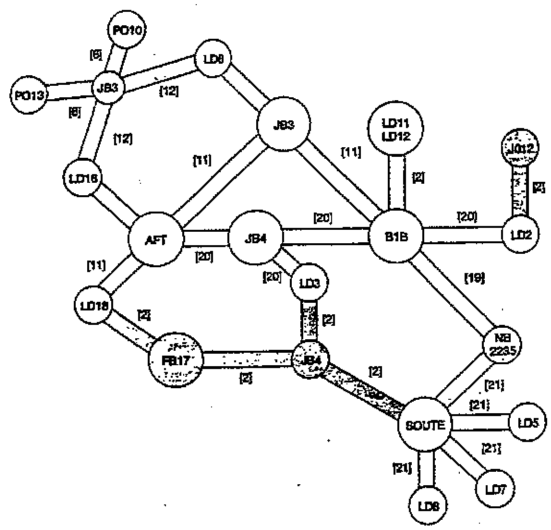

b. Transmission line network for the aircraft cable harness.

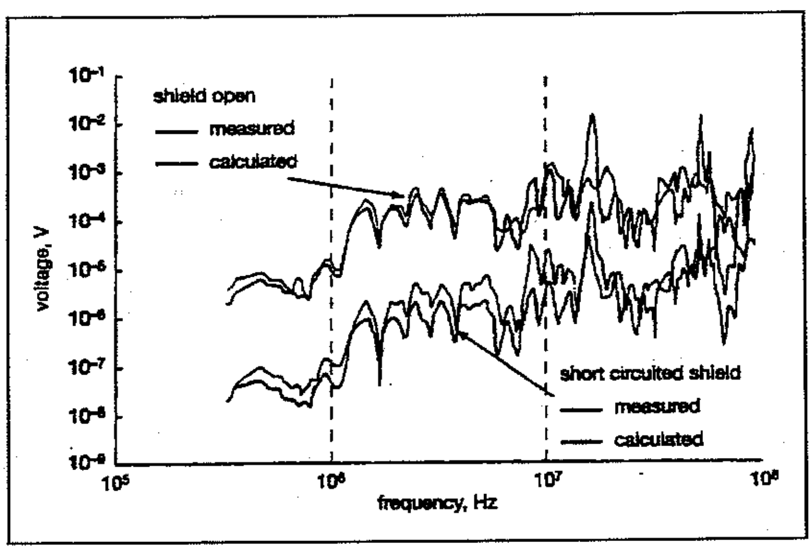

c. Comparison of measured and calculated cable voltages, shown as a function of frequency.

Figure 5. Illustration of the use of topological modeling concepts for cable responses within an aircraft (after Parmantier [13]).

Parmantier's work on the modeling of the aircraft cable harness was directed towards a NEMP analysis of the aircraft equipment response, and consequently, neglecting the EM field coupling paths is a reasonable assumption. However, in attempting to apply these topological models to higher frequencies that are typical of HPM or the UWB threats, it becomes desirable to include these additional field-coupling paths in the BLT equation.

To show what is desired in this regard, consider the diagram in Figure 6, which shows a simple enclosure with an external antenna with a conducting penetration, and an aperture penetration. An external EM source produces an incident field that couples to the antenna, producing currents and charges that penetrate into the system interior by propagation along the conductors (the solid lines). In addition, the incident field is able to penetrate through the aperture, and then propagate to the interior, where it couples to an internal conductor. This field propagation is indicated by the dotted lines in the figure. Both of these coupling paths provide a response at an internal load point.

The conventional BLT equation describes the propagation of EM energy (in the form of voltage or current) along the conductors only, with the excitation arising from knowledge of the excitation EM field acting on the antenna. A more general form of the BLT equation can be envisioned that models the propagation of EM energy *both* on the conductors and through space, with the excitation function now being a specification of the fundamental radiation properties of the external EM source – not just an incident EM field on the system. In this way, a more complete EM interaction model results, and its responses are expected to be more accurate at the higher frequencies.

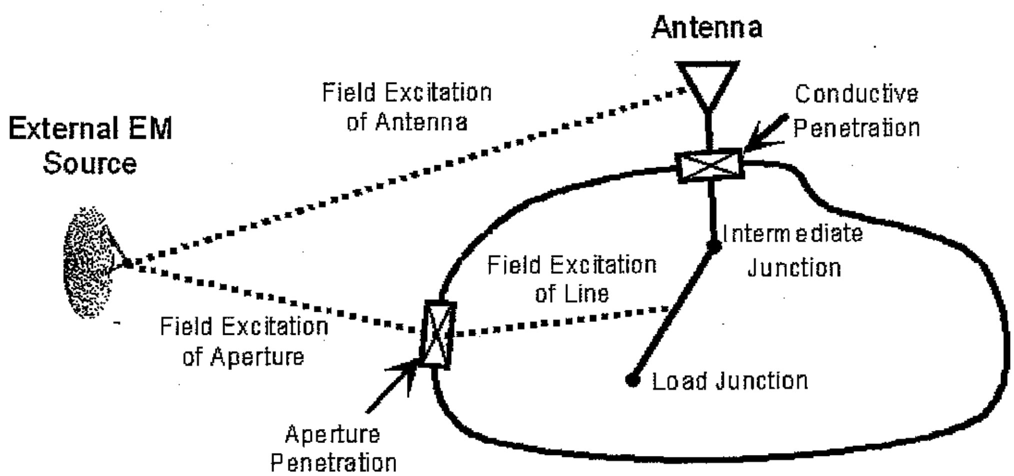

Figure 6. A simple example of a more general interaction path, containing both EM field and hard-wired interaction paths.

This report serves to outline the approach to be taken to extend the BLT equation to account for the effects of EM field propagation within the system. We take a top-level approach to show the general extension to the model, and in doing so, we neglect a number of effects that can be of importance in the application of this model to real systems. Specifically, we

- Neglect the near-field effects in the behavior of the source and the transmission lines. In doing so, only the far-field plane-wave relationships for the coupling and scattering of the elements in the model are considered.

- Neglect the possibility of different polarizations of the EM fields

- Neglect the possibility of the existence of a common mode (or "antenna" mode) response on the transmission lines. This implies that only the transmission line mode is considered, which is suitable for the case when the conductor is located over a reference groundplane.

- Neglect the higher order modes that can exist on the conductors, and assume that the coupled EM field responses (the line current and charge) are adequately represented by transmission line theory.

- Assume that the scattered EM field from any of the conductors within the network is adequately modeled from knowledge of the currents obtained from transmission line theory.

What we concentrate on in this paper is the manner in which the BLT equation must be modified to take into account the field coupling. While including all of the above effects would certainly be possible, we believe that they might obscure the main features of the BLT extensions, and consequently, these refinements are postponed for future discussion.

The starting point of the present paper is a short review of the derivation of the BLT equation for a simple section transmission line. This is done in Section 2, which provides an introduction to the BLT concept and shows how it can be applied to a more extensive network like that of Figure 4. Then, in Section 3 the steps necessary to extend the BLT equation to include the field coupling paths is described. This methodology is illustrated with a very simple example of a single dipole source coupling to a transmission line. In Section 4, the BLT theory is further extended to treat the problem of field coupling from a dipole source through an aperture to a transmission line and a simple example is given. Finally, in Section 5 these results are summarized and references are provided in Section 6. Appendices A and B contain further information on the field coupling and radiation functions for the transmission line structure used in the examples.

It should be noted that there are no numerical calculations or illustrations of this theory in the present paper. The goal of the discussion here is to outline the analysis methodology, and in doing so, many of the details of field polarization and spatial variations of the radiated or scattered fields are neglected. We anticipate that these details will be filled in at a later date in a companion paper that provides numerical demonstrations of this BLT formalism.

2. Review of the Derivation of the BLT Equation

To begin the development of the BLT equation containing distributed EM field signal paths and excitations, let us first review the basic steps used in deriving the conventional BLT equation for transmission line networks. Instead of treating a general transmission line network, however, we outline the formulation of the equation for a *single* transmission line, as shown in Figure 7. This development will shown the overall analysis approach, which can be generalized for a network of interconnected multiconductor transmission lines, as detailed in refs. [2] and [9]. This analysis is conducted in the frequency domain, with an assumed time dependence of $e^{j\omega t}$. Recall also that we are limiting our discussion to transmission line currents only: the antenna mode is not considered here. Physically this implies that we are considering a single conductor line located over a groundplane, with the image conductor in the groundplane serving as the second conductor in the 2-wire line.

The geometry shown in Figure 7 is that of a simple uniform two-wire transmission line of length L and characteristic impedance Z_c. We assume that it has a propagation constant γ, which in the most general case, can be dispersive if the line has resistive losses. The line is terminated at each end by impedance loads Z_{L1} and Z_{L2}, and it is assumed to be excited by a lumped voltage and/or current source, V_s and I_s, at the position $x = x_s$ along the line.

General expressions for the induced current $I(x)$ and voltage $V(x)$ at any position x along the line have been developed in [8]. In many instances, however, only the load voltages V_1 and V_2, or the corresponding load currents, are desired for the analysis. In this case, the results of performing an analysis for these load quantities can be put into a very compact form, known as the BLT equation.

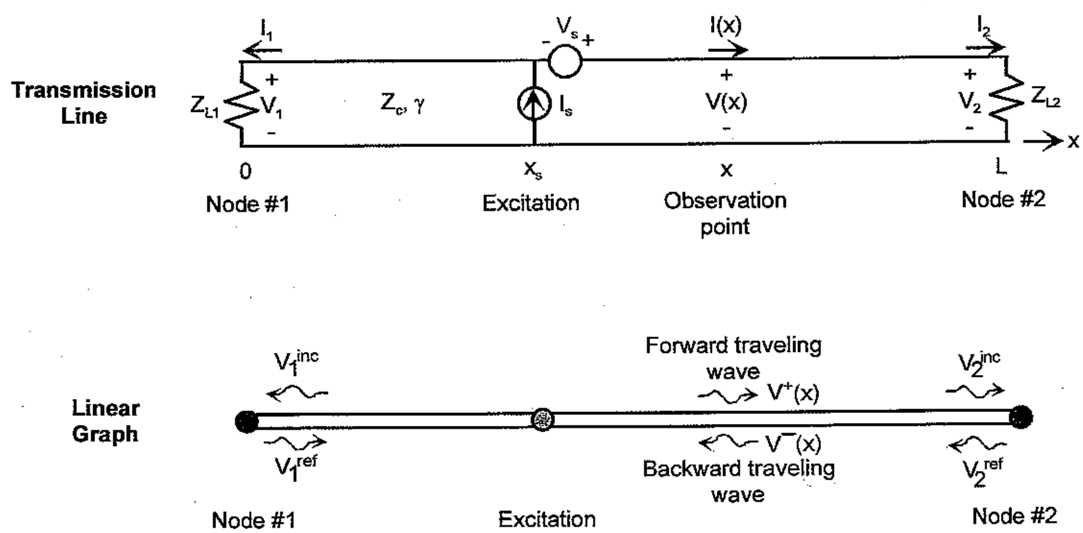

Figure 7. A simple transmission line with lumped source excitations (top) and its linear graph representation (bottom).

2.1 The Voltage BLT Equation

While a BLT equation can be developed for either the load voltages or the load currents, this development will concentrate on the equation for the voltage responses. The starting point of this analysis is to recognize that there are voltage *traveling waves* propagating in the positive direction (V^+) and in the negative direction (V^-), as shown in the bottom portion of Figure 7. Application of transmission line theory to this problem shows that these waves propagate on the line with a functional dependence of $e^{\mp\gamma x}$, respectively, and at any location x along the line, the total line voltage is calculated as the sum of the traveling waves, $V(x) = V^+(x) + V^-(x)$. The term γ is the propagation constant of the waves along the transmission line, which to first order is equal to $jk = j2\pi f/c$, which is the propagation constant of waves in free-space.

As noted in Figure 7, it is also useful to consider describing the voltage waves at the junctions by the *incident* and *reflected* voltage waves, V^{inc} and V^{ref}. Note that at nodes 1 and 2 of the simple transmission line graph, we have the following definitions:

$$V^+(0) \equiv V_1^+ = V_1^{ref} \;\; ; \;\; V^-(0) \equiv V_1^- = V_1^{inc} \quad \text{(at node 1)} \qquad (1a)$$

$$V^+(L) \equiv V_2^+ = V_2^{inc} \;\; ; \;\; V^-(L) \equiv V_2^- = V_1^{ref} \quad \text{(at node 2)} \qquad (1b)$$

For this simple transmission line, the voltage waves are initially excited by the lumped voltage and current source at $x = x_S$. As suggested in Figure 8 the sources produce a positive traveling wave for $x > x_S$ and a negative traveling wave for $x < x_S$. Ref. [8] derives expressions for these voltage waves in terms of the source strengths as

$$V_s^+(x) = \frac{1}{2}\left(V_s + Z_c I_s\right)e^{-\gamma(x-x_s)} \;\; ; \;\; V_s^-(x) = 0 \quad (\text{for } x > x_s) \qquad (2a)$$

$$V_s^-(x) = \frac{-1}{2}\left(V_s - Z_c I_s\right)e^{+\gamma(x-x_s)} \;\; ; \;\; V_s^+(x) = 0 \quad (\text{for } x < x_s) \qquad (2b)$$

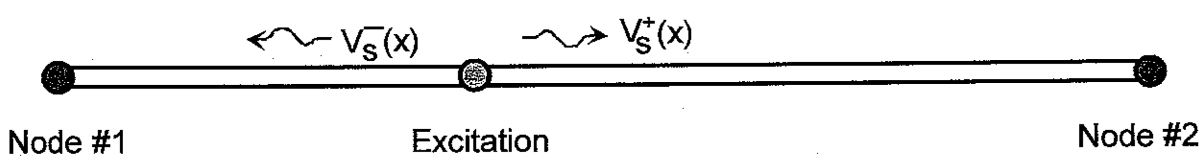

Figure 8. Illustration of the positive and negative traveling waves excited by the lumped sources at $x = x_S$.

With no excitation sources, the positive traveling voltage at junction #2 is expressed in terms of the positive traveling wave at junction #1 as

$$V_2^+ = V_1^+ e^{-\gamma L}. \tag{3}$$

However, with the source present, there is an additional component to V_2^+ that is due to the positive wave traveling away from the source. In this manner, Eq.(3) is modified[2] to include the source terms, as

$$V_2^+ = V_1^+ e^{-\gamma L} + \frac{1}{2}(V_s + Z_c I_s)e^{-\gamma(L-x_s)}. \tag{4}$$

Similarly, the negative traveling wave at junction #1 may be expressed in terms of the negative wave at junction #2, plus the source contribution as

$$V_1^- = V_2^- e^{-\gamma L} - \frac{1}{2}(V_s - Z_c I_s)e^{-\gamma x_s}. \tag{5}$$

Expressing the voltage traveling waves in terms of the incident and reflected waves at the junctions using Eq.(1), Eqs.(4) and (5) can be put into a matrix equation for the *incident* waves at the two junctions as

$$\begin{bmatrix} V_1^{inc} \\ V_2^{inc} \end{bmatrix} = \begin{bmatrix} 0 & e^{-\gamma L} \\ e^{-\gamma L} & 0 \end{bmatrix} \cdot \begin{bmatrix} V_1^{ref} \\ V_2^{ref} \end{bmatrix} + \begin{bmatrix} -\frac{1}{2}(V_s - Z_c I_s)e^{-\gamma x_s} \\ \frac{1}{2}(V_s + Z_c I_s)e^{-\gamma(L-x_s)} \end{bmatrix}. \tag{6}$$

Rearranging the terms of Eq.(6) provides a similar expression for the *reflected* voltages at the loads:

$$\begin{bmatrix} V_1^{ref} \\ V_2^{ref} \end{bmatrix} = \begin{bmatrix} 0 & e^{\gamma L} \\ e^{\gamma L} & 0 \end{bmatrix} \cdot \begin{bmatrix} V_1^{inc} \\ V_2^{inc} \end{bmatrix} + \begin{bmatrix} -\frac{1}{2}(V_s + Z_c I_s)e^{\gamma x_s} \\ +\frac{1}{2}(V_s - Z_c I_s)e^{\gamma(L-x_s)} \end{bmatrix}. \tag{7}$$

Transmission line theory [8] provides a useful relationship between the incident and reflected voltage waves at a load through the expression

$$V^{ref} = \rho V^{inc}, \tag{8}$$

where ρ is the *voltage* reflection coefficient. For an impedance load Z_L on a transmission line having a characteristic impedance Z_c, the reflection coefficient is defined as

[2] In mathematical terms, this expression is viewed as a solution to the wave equation with sources, which contains a homogeneous solution and a particular solution.

$$\rho = \frac{Z_L - Z_c}{Z_L + Z_c}. \tag{9}$$

For this simple transmission line network, the vector of reflected voltages in Eq.(7) can be expressed in terms of the vector of incident voltages by the matrix relationship

$$\begin{bmatrix} V_1^{ref} \\ V_2^{ref} \end{bmatrix} = \begin{bmatrix} \rho_1 & 0 \\ 0 & \rho_2 \end{bmatrix} \cdot \begin{bmatrix} V_1^{inc} \\ V_2^{inc} \end{bmatrix}, \tag{10}$$

where ρ_1 and ρ_2 are the reflection coefficients at each end (node) of the line.

Substituting Eq.(10) into Eq.(7) and solving for the vector of incident voltages provides the first form of the voltage BLT equation:

$$\begin{bmatrix} V_1^{inc} \\ V_2^{inc} \end{bmatrix} = \left\{ \begin{bmatrix} 0 & e^{\gamma L} \\ e^{\gamma L} & 0 \end{bmatrix} - \begin{bmatrix} \rho_1 & 0 \\ 0 & \rho_2 \end{bmatrix} \right\}^{-1} \cdot \begin{bmatrix} \frac{1}{2}(V_s + Z_c I_s) e^{\gamma x_s} \\ -\frac{1}{2}(V_s - Z_c I_s) e^{\gamma (L - x_s)} \end{bmatrix}, \tag{11}$$

or upon combining the terms of the inverted matrix,

$$\begin{bmatrix} V_1^{inc} \\ V_2^{inc} \end{bmatrix} = \begin{bmatrix} -\rho_1 & e^{\gamma L} \\ e^{\gamma L} & -\rho_2 \end{bmatrix}^{-1} \cdot \begin{bmatrix} \frac{1}{2}(V_s + Z_c I_s) e^{\gamma x_s} \\ -\frac{1}{2}(V_s - Z_c I_s) e^{\gamma (L - x_s)} \end{bmatrix}. \tag{12}$$

This is an equation for the incident voltage waves at both ends of the line, in terms of the transmission line parameters, the load impedances and the source excitations.

The second form of the voltage BLT equation is for the *total* load voltage vector, which is obtained using Eq. (10), as

$$\begin{aligned} \begin{bmatrix} V_1 \\ V_2 \end{bmatrix} &= \begin{bmatrix} V_1^{inc} \\ V_2^{inc} \end{bmatrix} + \begin{bmatrix} V_1^{ref} \\ V_2^{ref} \end{bmatrix} \\ &= \left\{ \begin{bmatrix} 1 & 0 \\ 0 & 1 \end{bmatrix} + \begin{bmatrix} \rho_1 & 0 \\ 0 & \rho_2 \end{bmatrix} \right\} \cdot \begin{bmatrix} V_1^{inc} \\ V_2^{inc} \end{bmatrix} \\ &= \begin{bmatrix} 1+\rho_1 & 0 \\ 0 & 1+\rho_2 \end{bmatrix} \cdot \begin{bmatrix} V_1^{inc} \\ V_2^{inc} \end{bmatrix} \end{aligned} \tag{13}$$

Substituting this expression into Eq.(12) yields the following total voltage BLT equation:

$$\begin{bmatrix} V_1 \\ V_2 \end{bmatrix} = \begin{bmatrix} 1+\rho_1 & 0 \\ 0 & 1+\rho_2 \end{bmatrix} \cdot \begin{bmatrix} -\rho_1 & e^{\gamma L} \\ e^{\gamma L} & -\rho_2 \end{bmatrix}^{-1} \cdot \begin{bmatrix} S_1 \\ S_2 \end{bmatrix}, \tag{14}$$

where the source (excitation) term for the lumped current and/or voltage sources at $x = x_S$ is defined as

$$\begin{bmatrix} S_1 \\ S_2 \end{bmatrix} = \begin{bmatrix} \frac{1}{2}(V_s + Z_c I_s)e^{\gamma x_s} \\ -\frac{1}{2}(V_s - Z_c I_s)e^{\gamma(L-x_s)} \end{bmatrix}. \tag{15}$$

Note that S_1 represents the source term for the excitation of the positive traveling voltage wave on the line, while S_2 denotes the source excitation for the negative traveling voltage wave.

2.2 The Current BLT Equation

A similar analysis involving current traveling waves can be used to derive a BLT equation for the currents flowing in the load impedances of the line. In doing so, care must be used in accounting for the difference in sign between the *line current* and the *load current* at the load at $x = 0$. Alternatively, one can use the load voltage BLT equation (14) and the V-I relationship at the loads to determine the load current. In any case, the following BLT equation for the loads currents results:

$$\begin{bmatrix} I_1 \\ I_2 \end{bmatrix} = \frac{1}{Z_c}\begin{bmatrix} 1-\rho_1 & 0 \\ 0 & 1-\rho_2 \end{bmatrix} \cdot \begin{bmatrix} -\rho_1 & e^{\gamma L} \\ e^{\gamma L} & -\rho_2 \end{bmatrix}^{-1} \cdot \begin{bmatrix} S_1 \\ S_2 \end{bmatrix}. \tag{16}$$

2.3 The BLT Equations for Incident Field Excitation

The BLT equations for the load voltages and currents due to lumped sources at $x = x_S$ derived in the previous sections can be used to determine the induced load responses arising from the illumination of the line by an incident EM field, as shown in Figure 9. As noted in [7] and [14], an incident EM field acting on a two-wire line can be thought of as producing voltage sources that are *distributed* along both of the wires of the line, as well as two lumped voltage sources at the line ends[3]. The distributed voltage sources induce both the antenna mode (which we neglect in this discussion) and the transmission line mode, which contributes to the load currents.

---

[3] This analysis is based on the so-called Agrawal formulation of the transmission line excitation and is formally valid for a transmission line in free space or in a homogeneous dielectric material. For the interesting case of a dielectric coated transmission line, the use of the Agrawal formulation is open to question, and is a current problem of interest in transmission line theory.

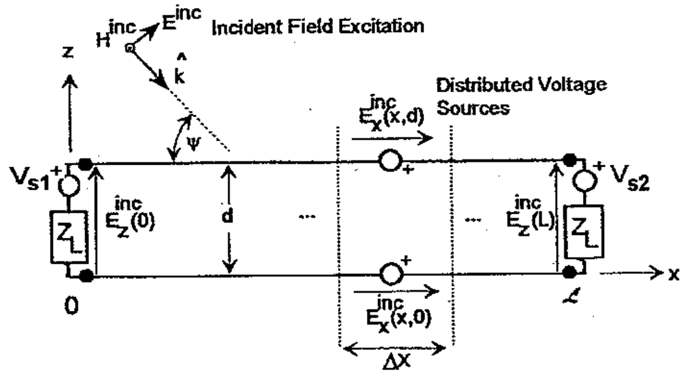

Figure 9. Field excitation of a two-wire transmission line, showing the voltage excitation sources needed in the BLT equation.

The derivation of the field coupling to the simple two-wire line is presented in Appendix A, where it is shown that the same BLT equations (14) and (16) for the load voltages and currents can be used to describe the field coupling responses, but with a different source vector. Assuming that the propagation constant on the line is the same as that of free space ($\gamma = jk = j\omega/c$), this source vector is found by integrating the effects of the distributed field sources along the line and combining the effects of the end sources.

For the special case of the incident field being a plane wave with an angle of incidence ψ and the incident E-field lying in the plane of the transmission line, the resulting source term has the following form[4]:

$$\begin{bmatrix} S_1 \\ S_2 \end{bmatrix} = \frac{E^{inc} d}{2} \begin{bmatrix} \left(e^{jkL(1-\cos\psi)} - 1\right) \\ e^{jkL}\left(e^{-jkL(1+\cos\psi)} - 1\right) \end{bmatrix} . \qquad (17)$$
$$\equiv E^{inc} \begin{bmatrix} F_1(\psi) \\ F_2(\psi) \end{bmatrix}$$

Inserting Eq.(17) into Eq.(14) or (16) thus provides the load responses for plane wave excitation of the line.

2.4 Generalized Forms for the BLT Equations

In examining the derivation of the BLT equation for the single transmission line, it is possible to illustrate the forms that the solutions take for more general networks or for

---

[4] Ref.[8] presents the more general expression for this source vector for the case of an arbitrarily incident and polarized EM field acting on the line, and for the case of the transmission line propagation constant γ differing from the free space propagation constant, jk. This results in a more complicated expression for the excitation terms.

multiconductor transmission lines. Consider the definitions of the following terms, which have been used in the previous sections:

<u>Line Propagation Matrix</u>
$$\overline{\overline{\Gamma}} = \begin{bmatrix} 0 & e^{\gamma L} \\ e^{\gamma L} & 0 \end{bmatrix} \tag{18}$$

<u>Load Scattering Matrix</u>
$$\overline{\overline{S}} = \begin{bmatrix} \rho_1 & 0 \\ 0 & \rho_2 \end{bmatrix} \tag{19}$$

<u>Characteristic Admittance Matrix</u>
$$\overline{\overline{Y}}_c = \begin{bmatrix} 1/Z_c & 0 \\ 0 & 1/Z_c \end{bmatrix} \tag{20}$$

<u>Unit Matrix</u>
$$\overline{\overline{U}} = \begin{bmatrix} 1 & 0 \\ 0 & 1 \end{bmatrix}. \tag{21}$$

<u>Response Vectors</u>
$$\overline{V} = \begin{bmatrix} V_1 \\ V_2 \end{bmatrix} \; ; \; \overline{I} = \begin{bmatrix} I_1 \\ I_2 \end{bmatrix} \tag{22}$$

With these definitions, the total voltage BLT equation (14) takes the shorthand form

$$\overline{V} = \left[\overline{\overline{U}} + \overline{\overline{S}}\right] \cdot \left[\overline{\overline{\Gamma}} - \overline{\overline{S}}\right]^{-1} \cdot \overline{E} \tag{23}$$

and the corresponding current BLT equation is

$$\overline{I} = \overline{\overline{Y}}_c \left[\overline{\overline{U}} - \overline{\overline{S}}\right] \cdot \left[\overline{\overline{\Gamma}} - \overline{\overline{S}}\right]^{-1} \cdot \overline{E}. \tag{24}$$

As discussed in [9] the BLT equation for a network of interconnected transmission lines has the same form as Eq.(23) or (24). The matrix $\overline{\overline{\Gamma}}$ represents all of the propagation functions (in the forward and backward directions) on each of the transmission lines in the network. Thus, if there are N transmission lines (sometimes called "tubes") in the network, then $\overline{\overline{\Gamma}}$ is of order $2N \times 2N$. Assuming that the responses are ordered according to the tube number in the network, $\overline{\overline{\Gamma}}$ is a block diagonal matrix, with each sub-matrix defining the propagation terms for the individual transmission lines.

The scattering matrix $\overline{\overline{S}}$ contains all of the scattering coefficients from all of the junctions in the network. For the responses ordered by the tube number, this matrix is sparse, but not necessarily block diagonal, since the locations of the various scattering coefficients depend on how the junctions in the network are numbered and interconnected.

3. Extension of the BLT Equation for Distributed Field Excitation

In goal of this paper is to extend the concept of the transmission line network and its solution via the BLT equation to the distributed field problem shown in Figure 10. This configuration consists of a source of EM energy located outside a shielded enclosure, which contains an internal transmission line. Generally, in the external and internal regions there can be other scattering objects that influence the fields. The shield is assumed to have a small aperture; the EM fields that leak through this aperture are able to induce currents and charge on the wire and the load voltage and current responses are to be determined. Reference [15] has discussed one aspect of this problem, and here we will develop an alternate approach that is consistent with the assumptions of transmission line theory.

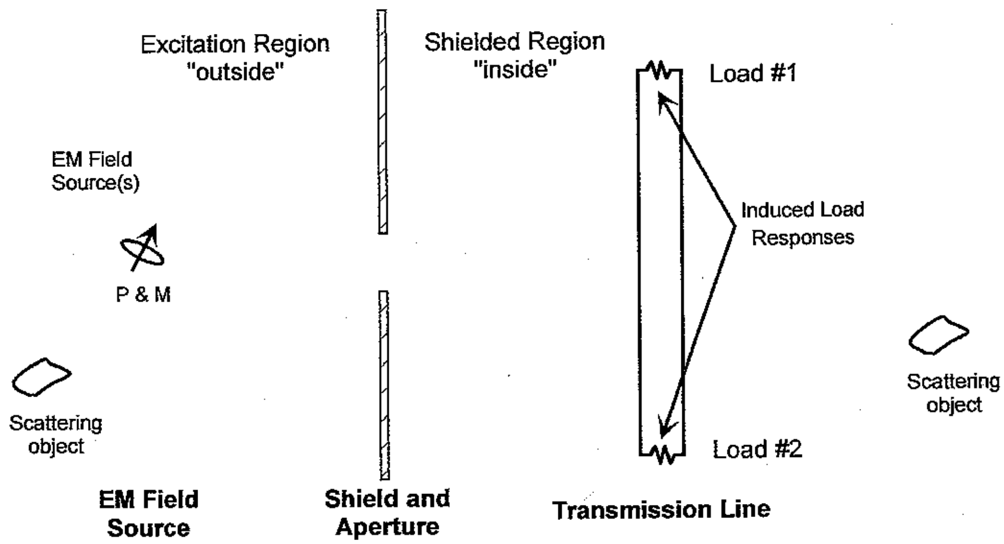

Figure 10. Problem geometry for an external EM field source producing a current response on a transmission line within a shielded region.

As mentioned earlier, we are not interested in providing a detailed numerical solution at this stage. Consequently, we will ignore many of the (important) subtleties of such an EM analysis, including EM field polarization and angle of incidence, geometrical details of the shield and aperture, source details (radiation pattern, etc.), and the fact that antenna modes can be induced on the transmission line structure in addition to the transmission line modes. We wish to avoid these details and concentrate on the basic concepts of extending the BLT equation to be able to treat EM field propagation and coupling.

Following the development of the BLT equation, as summarized in Section 2, we wish to describe the EM interaction problem of Figure 10 using a description of traveling waves on appropriate tubes (or branches) and reflection coefficients at the appropriate junction (or nodes) within the problem volume. As is evident from this figure, in some parts of the problem, the traveling waves can describe electromagnetic fields that propagate from one point in space to another. Traveling waves also exist on the transmission line, and in this case, they are best described by voltage and current disturbances, rather than by EM fields. These latter traveling waves are those already treated by the conventional BLT equation.

Similarly, at some locations in the problem, reflections can be represented by EM field reflection coefficients, and at other locations, transmission line voltage or current reflection coefficients are appropriate.

A fundamental issue in developing a BLT representation for the interaction problem of Figure 10 is how to treat the EM field coupling between the incident field and the transmission line. To this end, it is prudent to solve a simple, preliminary problem that shows how this coupling can be incorporated into the BLT equation, and then later consider the solution to the more complex problem of Figure 10.

To this end, the simple source/transmission line problem shown in Figure 11 can be considered. A simple transmission line having load specified at each end is illuminated by a distant electrical source, which induces currents and voltages at the loads. In this simple example, we neglect the presence of the scattering objects shown in Figure 10, and concentrate only on the excitation of the transmission line and its re-radiation.

By knowing the incident E-field E^{inc} at the transmission line, the BLT equations (14) or (16), together with the excitation terms in Eq.(17) can be used directly to determine the load responses (for assumed plane wave excitation). In this manner, the incident E-field is considered to be the primary excitation of the problem (as this excitation occurs in the "forcing" term of the BLT equation.

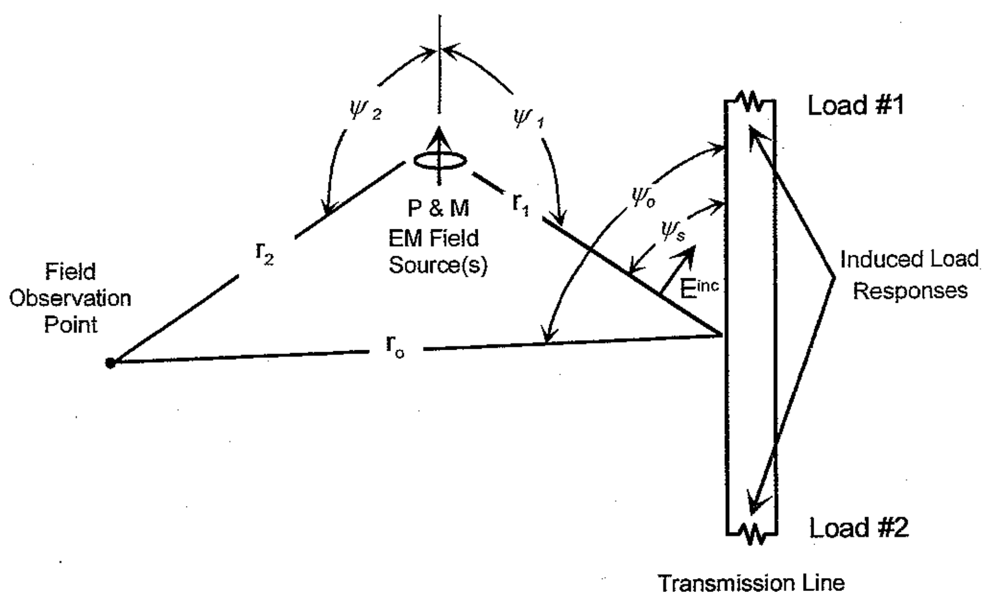

Figure 11. Geometry of a simple elementary source exciting a transmission line.

What we desire, however, is to consider the excitation in the problem shown in Figure 11 to be the dipole sources themselves $\left(\vec{P} \text{ and } \vec{M}\right)$, not the incident fields they produce. In this way, the incident field on the transmission line, along with a scattered EM field from the line will constitute additional response variables in an expanded BLT equation.

The analysis of this simple problem can be described in terms of the signal flow diagram illustrated in Figure 12, which shows the paths of energy flow. The transmission line is represented by the "conventional" tube with solid lines and is denoted as Tube 1. This is identical to the usual tubes used in the BLT equation, with forward and backward propagating voltage and current waves. Nodes 1 and 2 represent the transmission line loads, as described in Section 2, and these are represented by reflection coefficients relating the incident and reflected voltage and current waves at these locations.

In addition to the transmission line tube, there is an EM field propagation "tube", which is denoted by the dotted lines. This is Tube 2 and it represents the path by which the EM field propagates from the source to the line (at node 4), and also to a distant field observation point, at node 3. At these nodes, the responses that are to be included in the BLT equation are the E and H fields.

Nodes 1, 2 and 3 can be thought of as conventional nodes, in which there are incident and reflected voltages and currents (or E and H-fields). The field node 3 is really not of interest here, because it might be thought of as being "at infinity" with a zero reflection coefficient to represent outward only propagation of the EM fields in free space. However, in more complicated problems, this node may be important, say if there were an electrical conducting wall or other object far from the source and transmission line. Thus, this node will remain in the sample problem discussed here.

Node 4 is a different type of node from the others, in that it contains the EM field coupling and scattering information for this problem. Consequently, it is represented by a different type of node symbol – a box rather than a circle. At this node, there is an incident EM field component produced by the dipole sources, as well as a reflected EM field from node 3. This incident EM field is "reflected" by the transmission line structure, and results in a scattered EM field propagating away towards node 3. At the same time, this incident EM field on the line contributes to the incident voltage and current waves at the transmission line nodes 1 and 2. Furthermore, the reflected voltage and current waves from nodes 1 and 2 are able to re-radiate, and this produces a component of the scattered EM field from the transmission line.

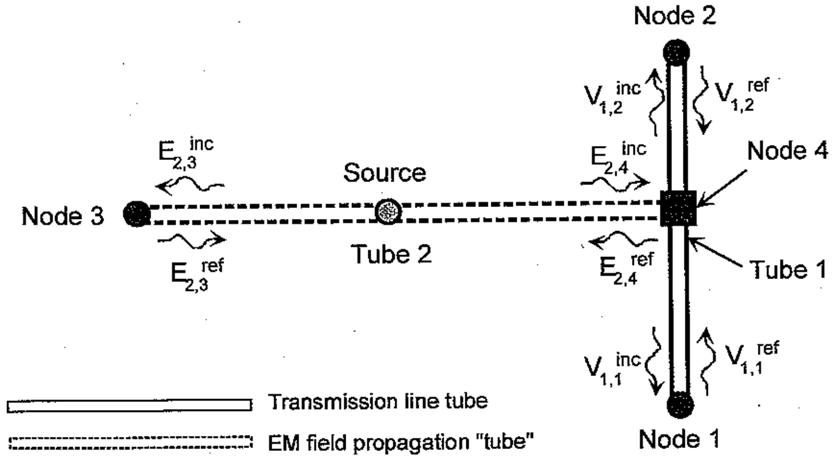

Figure 12. The signal flow graph for the EM interaction geometry of Figure 11.

To begin with the development of the modified BLT equation, we will first clarify a notational issue. A traveling wave component (voltage, current, E-field, or H-field) will be found on each tube *i* and at each node *j* of the network. This will be represented using the notation $R_{i,j}$. Moreover, for this problem, we will concentrate on voltage and E-field responses (with the corresponding current and H-field responses being obtained from characteristic impedances of the transmission line and free space).

To develop the network BLT equation, we will need to examine both the tube propagation relationships and the node reflection relationships, as described in the next section.

3.1 Tube Propagation Relationships

Considering first the transmission line Tube 1, the relationship between the reflected and incident voltages at nodes 1 and 2 can be expressed from Eq.(7) as

$$\begin{bmatrix} V_{1,1}^{ref} \\ V_{1,2}^{ref} \end{bmatrix} = \begin{bmatrix} 0 & e^{\gamma L} \\ e^{\gamma L} & 0 \end{bmatrix} \cdot \begin{bmatrix} V_{1,1}^{inc} \\ V_{1,2}^{inc} \end{bmatrix} + \begin{bmatrix} -F_1(\psi_s)E_{2,4}^{inc} \\ -F_2(\psi_s)E_{2,4}^{inc} \end{bmatrix}, \qquad (25)$$

where the effects of the incident E-field at the wire ($E_{2,4}^{inc}$) can be represented by the integral functions $F_1(\psi_s)$ and $F_2(\psi_s)$ developed in Appendix A. Note that these functions depend on the local angle of incidence at the line ψ_s and in the more general case, on the polarization angles. Note that Eq.(25) contains two terms. The first is a propagation relationship between incident and reflected voltage waves on the transmission line having a propagation constant γ. The second is a term that relates to the excitation of waves on the line due to the incident field $E_{2,4}^{inc}$.

A similar equation for incident and reflected E-fields in tube 2 can be developed. Neglecting polarization issues, the incident field at node 4 can be expressed as

$$E_{2,4}^{inc} = \frac{a_3 e^{-jkr_o}}{r_o} E_{2,3}^{ref} + \mathcal{S}_1(\psi_1)\frac{e^{-jkr_1}}{r_1} \tag{26}$$

where the terms e^{-jkr}/r take into account the spherical propagation of fields through space and $\mathcal{S}_1(\psi_1)$ denotes the amplitude and angular source term from the elementary dipole sources, which are the primary sources in this example. The term ψ_1 represents the angle of departure of the radiation from the source to the transmission line, relative to some convenient source axis, as noted in Figure 11. Furthermore, the term a_3 in Eq.(26) represents a typical dimension of the scattering body at node 3.

Similarly, at node 3, the propagation relationship for the incident E-field $E_{2,3}^{inc}$ can be expressed as

$$E_{2,3}^{inc} = \frac{a_4 e^{-jkr_o}}{r_o} E_{2,4}^{ref} + \mathcal{S}_2(\psi_2)\frac{e^{-jkr_2}}{r_2} + \frac{jk}{2\pi}\frac{Z_o}{Z_c}\frac{e^{-jkr_o}}{r_o}\left(F_1(\psi_o)V_{1,1}^{inc} + F_2(\psi_o)V_{1,2}^{inc}\right). \tag{27}$$

The source term $\mathcal{S}_2(\psi_2)$ in this expression is the same as in Eq.(26), but with a different intensity because the observation angle ψ_2 and distance from the source to node 3 is different than from node 4. The incident field at node 3, $E_{2,3}^{inc}$, also contains source components from the traveling waves existing on the transmission line, as developed in Appendix A, by way of the F_1 and F_2 functions. The term a_4 denotes the overall size of the node 4, which is needed for dimensional consistency.

Eqs.(26) and (27) can be put into matrix form as

$$\begin{bmatrix} E_{2,3}^{inc} \\ E_{2,4}^{inc} \end{bmatrix} = \begin{bmatrix} 0 & \dfrac{a_4 e^{-jkr_o}}{r_o} \\ \dfrac{a_3 e^{-jkr_o}}{r_o} & 0 \end{bmatrix} \cdot \begin{bmatrix} E_{2,3}^{ref} \\ E_{2,4}^{ref} \end{bmatrix} + \frac{jk}{2\pi}\frac{Z_o}{Z_c}\frac{e^{-jkr_o}}{r_o}\begin{bmatrix} F_1(\psi_0) & F_2(\psi_0) \\ 0 & 0 \end{bmatrix} \cdot \begin{bmatrix} V_{1,1}^{inc} \\ V_{1,2}^{inc} \end{bmatrix} + \begin{bmatrix} \mathcal{S}_2(\psi_2)\dfrac{e^{-jkr_2}}{r_2} \\ \mathcal{S}_1(\psi_1)\dfrac{e^{-jkr_1}}{r_1} \end{bmatrix} \tag{28}$$

and upon rearranging terms, this equation can be solved for the *reflected* fields at the nodes as

$$\begin{bmatrix} E_{2,3}^{ref} \\ E_{2,4}^{ref} \end{bmatrix} = \begin{bmatrix} 0 & \dfrac{r_o e^{jkr_o}}{a_3} \\ \dfrac{r_o e^{jkr_o}}{a_4} & 0 \end{bmatrix} \begin{bmatrix} E_{2,3}^{inc} \\ E_{2,4}^{inc} \end{bmatrix} - \frac{jk}{2\pi a_4}\frac{Z_o}{Z_c}\begin{bmatrix} 0 & 0 \\ F_1(\psi_o) & F_2(\psi_o) \end{bmatrix} \begin{bmatrix} V_{1,1}^{inc} \\ V_{1,2}^{inc} \end{bmatrix} - \begin{bmatrix} \dfrac{\mathcal{S}_1(\psi_1)}{a_3}\dfrac{r_o e^{jk(r_o - r_1)}}{r_1} \\ \dfrac{\mathcal{S}_2(\psi_2)}{a_4}\dfrac{r_o e^{jk(r_o - r_2)}}{r_2} \end{bmatrix}. \tag{29}$$

Combining the propagation portions of Eq.(25) and Eq.(29) into a single 4 × 4 matrix for the reflected quantities provides the following propagation equation for this composite problem:

$$\begin{bmatrix} V_{1,1}^{ref} \\ V_{1,2}^{ref} \\ E_{2,3}^{ref} \\ E_{2,4}^{ref} \end{bmatrix} = \begin{bmatrix} 0 & e^{\gamma L} & 0 & -F_1(\psi_s) \\ e^{\gamma L} & 0 & 0 & -F_2(\psi_s) \\ 0 & 0 & 0 & \frac{r_o e^{jkr_o}}{a_3} \\ -\frac{jk}{2\pi a_4}\frac{Z_o}{Z_c}F_1(\psi_o) & -\frac{jk}{2\pi a_4}\frac{Z_o}{Z_c}F_2(\psi_o) & \frac{r_o e^{jkr_o}}{a_4} & 0 \end{bmatrix} \cdot \begin{bmatrix} V_{1,1}^{inc} \\ V_{1,2}^{inc} \\ E_{2,3}^{inc} \\ E_{2,4}^{inc} \end{bmatrix} + \begin{bmatrix} 0 \\ 0 \\ -\frac{S_1(\psi_1)}{a_3}\frac{r_o e^{jk(r_o-r_1)}}{r_1} \\ -\frac{S_2(\psi_2)}{a_4}\frac{r_o e^{jk(r_o-r_2)}}{r_2} \end{bmatrix}. \qquad (30a)$$

Notice that the equation contains the information about how voltage wave propagate on the transmission line, how the E-fields propagate in free space, how the fields couple to the transmission line, and how the transmission line currents produce a radiated field.

Eq.(30a) is seen to have incident and reflected variables that are of mixed units: volts and volts/meter. This equation can be put into a more consistent form involving only the units of volts, by multiplying the last two rows of the equation by a_3 and a_4, respectively. This yields the following expression:

$$\begin{bmatrix} V_{1,1}^{ref} \\ V_{1,2}^{ref} \\ a_3 E_{2,3}^{ref} \\ a_4 E_{2,4}^{ref} \end{bmatrix} = \begin{bmatrix} 0 & e^{\gamma L} & 0 & -\frac{F_1(\psi_s)}{a_4} \\ e^{\gamma L} & 0 & 0 & -\frac{F_2(\psi_s)}{a_4} \\ 0 & 0 & 0 & \frac{r_o}{a_4} e^{jkr_o} \\ -\frac{jk}{2\pi}\frac{Z_o}{Z_c}F_1(\psi_o) & -\frac{jk}{2\pi}\frac{Z_o}{Z_c}F_2(\psi_o) & \frac{r_o}{a_3} e^{jkr_o} & 0 \end{bmatrix} \cdot \begin{bmatrix} V_{1,1}^{inc} \\ V_{1,2}^{inc} \\ a_3 E_{2,3}^{inc} \\ a_4 E_{2,4}^{inc} \end{bmatrix} + \begin{bmatrix} 0 \\ 0 \\ -S_1(\psi_1)\frac{r_o e^{jk(r_o-r_s)}}{r_s} \\ -S_2(\psi_2)\frac{r_o e^{jk(r_o-r_1)}}{r_1} \end{bmatrix}. \qquad (30b)$$

3.2 Node Reflection Relationships

Following the procedure used for the simple transmission line in Section 2, we now develop an expression for the reflected waves using the node parameters. At nodes 1 and 2, the relationships between the incident and reflected voltages are given by the reflection coefficients on the transmission line, involving the characteristic impedance Z_c of the line and the load impedance Z_L, as

$$V_{1,j}^{ref} = \rho_j V_{1,j}^{inc} \quad j = 1,2 \qquad (31)$$

with

$$\rho_i = \frac{Z_{Li} - Z_c}{Z_{Li} + Z_c} . \tag{32}$$

Similarly, at node 3, the E-field relationship is

$$E_{2,3}^{ref} = \rho_3 E_{2,3}^{inc} , \tag{33}$$

where ρ_3 now relates incident and reflected E-fields at node 3. As previously mentioned, we assume that this node is at infinity and there is no field reflection at this point, so $\rho_3 = 0$.

The definition of the reflection coefficient at node 4, ρ_4, is less obvious than at node 3. At node 4, it is clear that an incident field at the node will be reflected by the transmission line. However, this effect is already accounted for in the propagation relationships of Eq.(30). The reflection coefficient at node 4, therefore, is the reflection coefficient *in the absence of the transmission line*. If the region to the right side of the line in Figure 11 is free space, then there will be no reflection of the incident field. However, if there is a local groundplane at some distance from node 4, there can be a reflection of the incident field, with a corresponding reflection coefficient being defined.

Taking all of the reflected terms into account, the network reflection matrix can now be written as

$$\begin{bmatrix} V_{1,1}^{ref} \\ V_{1,2}^{ref} \\ E_{2,3}^{ref} \\ E_{2,4}^{ref} \end{bmatrix} = \begin{bmatrix} \rho_1 & 0 & 0 & 0 \\ 0 & \rho_2 & 0 & 0 \\ 0 & 0 & \rho_3 & 0 \\ 0 & 0 & 0 & \rho_4 \end{bmatrix} \cdot \begin{bmatrix} V_{1,1}^{inc} \\ V_{1,2}^{inc} \\ E_{2,3}^{inc} \\ E_{2,4}^{inc} \end{bmatrix} \tag{34a}$$

or in terms of the normalized voltage variables,

$$\begin{bmatrix} V_{1,1}^{ref} \\ V_{1,2}^{ref} \\ a_3 E_{2,3}^{ref} \\ a_4 E_{2,4}^{ref} \end{bmatrix} = \begin{bmatrix} \rho_1 & 0 & 0 & 0 \\ 0 & \rho_2 & 0 & 0 \\ 0 & 0 & \rho_3 & 0 \\ 0 & 0 & 0 & \rho_4 \end{bmatrix} \cdot \begin{bmatrix} V_{1,1}^{inc} \\ V_{1,2}^{inc} \\ a_3 E_{2,3}^{inc} \\ a_4 E_{2,4}^{inc} \end{bmatrix} \tag{34b}$$

3.3 The Extended BLT Equations

Eqs.(30) and (34) can now be solved for the vector of incident waves at the nodes using exactly the same technique demonstrated in Eqs.(10) – (12). This provides the following *extended* BLT equation for the incident voltages and E-fields at the nodes:

$$\begin{bmatrix} V_{1,1}^{inc} \\ V_{1,2}^{inc} \\ a_3 E_{2,3}^{inc} \\ a_4 E_{2,4}^{inc} \end{bmatrix} = \begin{bmatrix} -\rho_1 & e^{\gamma L} & 0 & -\frac{1}{a_4}F_1(\psi_s) \\ e^{\gamma L} & -\rho_2 & 0 & -\frac{1}{a_4}F_2(\psi_s) \\ 0 & 0 & -\rho_3 & \frac{r_o}{a_4}e^{jkr_o} \\ -\frac{jk}{2\pi}\frac{Z_o}{Z_c}F_1(\psi_o) & -\frac{jk}{2\pi}\frac{Z_o}{Z_c}F_2(\psi_o) & \frac{r_o}{a_3}e^{jkr_o} & -\rho_4 \end{bmatrix}^{-1} \cdot \begin{bmatrix} 0 \\ 0 \\ S_1(\psi_1)\frac{r_o e^{jk(r_o-r_s)}}{r_s} \\ S_2(\psi_2)\frac{r_o e^{jk(r_o-r_1)}}{r_1} \end{bmatrix}. \quad (35)$$

Using Eq.(34) in the above expression then provides the following total voltage and E-field extended BLT equation:

$$\begin{bmatrix} V_{1,1} \\ V_{1,2} \\ a_3 E_{2,3} \\ a_4 E_{2,4} \end{bmatrix} = \begin{bmatrix} 1+\rho_1 & 0 & 0 & 0 \\ 0 & 1+\rho_2 & 0 & 0 \\ 0 & 0 & 1+\rho_3 & 0 \\ 0 & 0 & 0 & 1+\rho_4 \end{bmatrix} \cdot$$

$$\begin{bmatrix} -\rho_1 & e^{\gamma L} & 0 & -\frac{1}{a_4}F_1(\psi_s) \\ e^{\gamma L} & -\rho_2 & 0 & -\frac{1}{a_4}F_2(\psi_s) \\ 0 & 0 & -\rho_3 & \frac{r_o}{a_4}e^{jkr_o} \\ -\frac{jk}{2\pi}\frac{Z_o}{Z_c}F_1(\psi_o) & -\frac{jk}{2\pi}\frac{Z_o}{Z_c}F_2(\psi_o) & \frac{r_o}{a_3}e^{jkr_o} & -\rho_4 \end{bmatrix}^{-1} \cdot \begin{bmatrix} 0 \\ 0 \\ S_1(\psi_1)\frac{r_o e^{jk(r_o-r_1)}}{r_1} \\ S_2(\psi_2)\frac{r_o e^{jl(r_o-r_2)}}{r_2} \end{bmatrix} \quad (42)$$

4. Application of the Extended BLT Equation to a More Complex Problem

With the background information on the development of the BLT equation, and its extension to permit the inclusion of propagating E-fields near the transmission line signal paths, it is possible to consider the more complex problem suggested in Figure 10. Figure 13 defines the various distances and angles that enter into this problem. Note that in this case, the scattering bodies in the outside and inside regions are includes, and the effects of the scattered fields from these bodies are incorporated in the BLT equation.

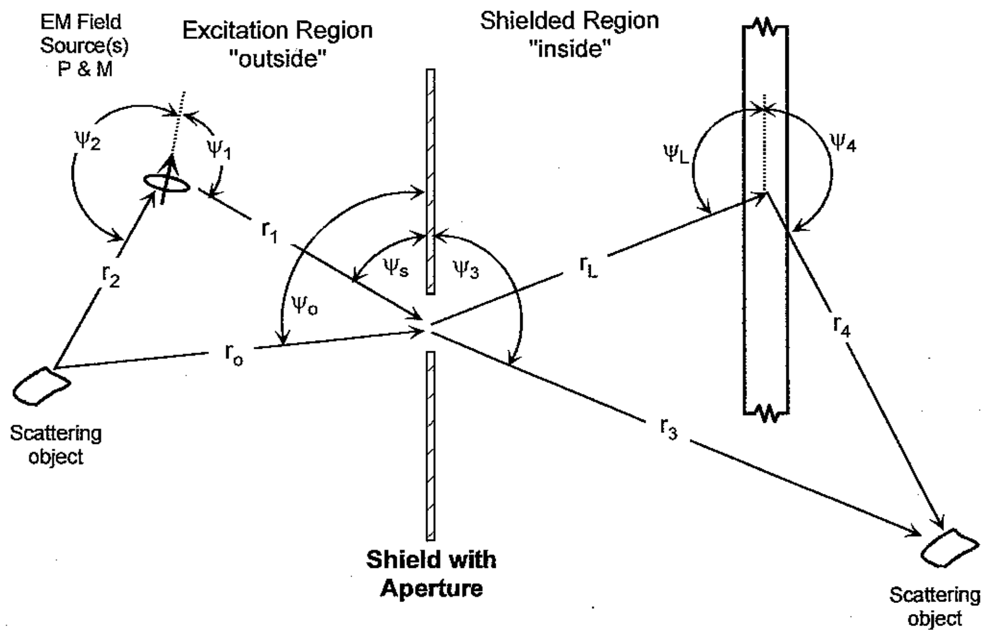

Figure 13. Geometry of the more general problem of Figure 10, showing relevant distances and angles.

For this more complex geometry, the signal flow diagram is shown in Figure 14. In this diagram, the various incident and reflected waves at the nodes in the network are illustrated. On the left of the diagram, Tube 2 represents the propagation path of EM fields in the region outside the shield. These fields are produced by an EM source, which we represent here simply as magnetic and electric dipole moments. This tube is connected to Node 3, which represents the scattering obstacle in the outside region, and to Node 4, which is the aperture in the conducting shield. This node acts much like a node in a transmission line network, in that it is represented by a scattering matrix that relates incident and reflected waves at the junction. Unlike the transmission line junction, however, the waves in this case are EM fields and not current or voltage waves on the lines.

As in the simple model in Figure 12, the transmission line is represented by Tube 1, with end Nodes 1 and 2. Tubes 3, 4 and 5 represent field propagation paths, and Node 6 is the other scattering object in the inside (shielded) region. As before, Node 5 is the field coupling node, in which there is an interaction between the incident fields on the line and the voltage traveling waves.

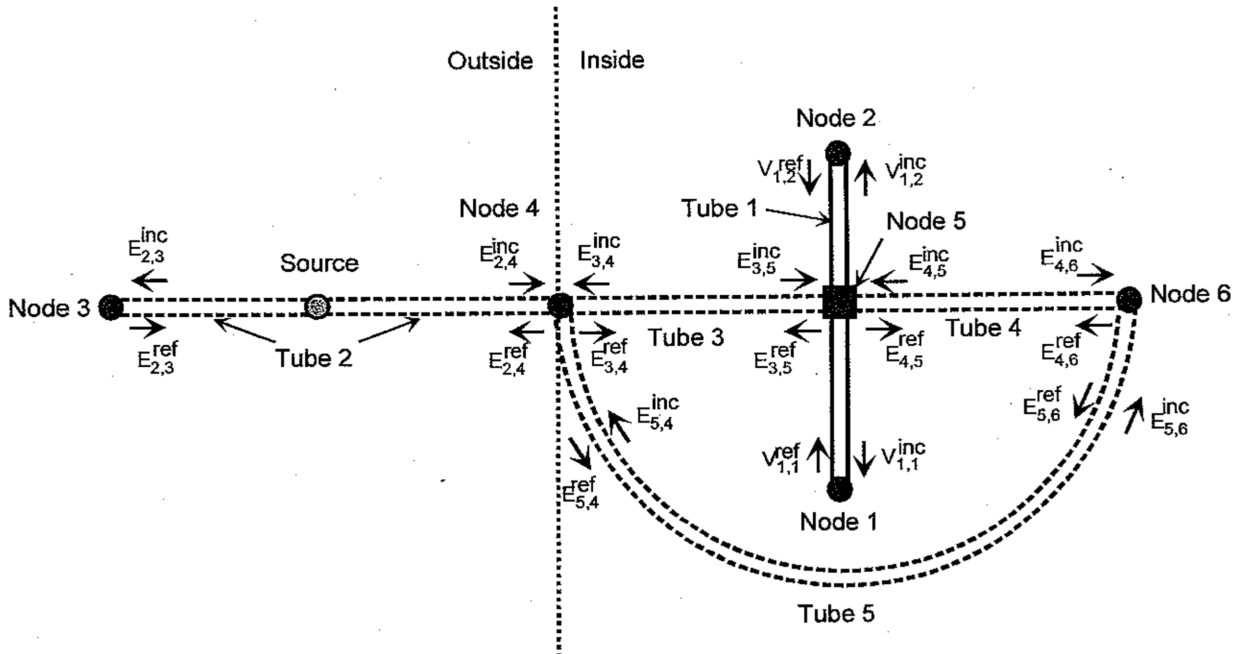

Figure 14. Signal flow diagram for the shielding problem of Figure 10.

Using the same analysis approach as in Section 3.3 for the field excited line, the reflected voltages on Tube 1 at Nodes 1 and 2 are given by the following expression, which is similar to Eq.(25). Note, however, that in this case there are two field coupling terns involving the incident E-fields from Tubes 3 and 4 and the coupling functions F_1 and F_2. Observe that these coupling terms are different in that they depend on the angles ψ_L and ψ_4, which are different as noted in Figure 13.

$$\begin{bmatrix} V_{1,1}^{ref} \\ V_{1,2}^{ref} \end{bmatrix} = \begin{bmatrix} 0 & e^{\gamma L} \\ e^{\gamma L} & 0 \end{bmatrix} \cdot \begin{bmatrix} V_{1,1}^{inc} \\ V_{1,2}^{inc} \end{bmatrix} + \begin{bmatrix} -F_1(\psi_L)E_{3,5}^{inc} \\ -F_2(\psi_L)E_{3,5}^{inc} \end{bmatrix} + \begin{bmatrix} -F_1(\psi_4)E_{4,5}^{inc} \\ -F_2(\psi_4)E_{4,5}^{inc} \end{bmatrix}, \tag{43}$$

For Tube 2, the relationship between the reflected and incident E-fields at nodes 3 and 4 are given by an equation similar to Eq.(29), but this time without the transmission line coupling excitation terms. This equation is presented in Eq.(44) and only the excitation effects of the primary sources are noted.

$$\begin{bmatrix} E_{2,3}^{ref} \\ E_{2,4}^{ref} \end{bmatrix} = \begin{bmatrix} 0 & \dfrac{r_o e^{jkr_o}}{a_3} \\ \dfrac{r_o e^{jkr_o}}{a_4} & 0 \end{bmatrix} \begin{bmatrix} E_{2,3}^{inc} \\ E_{2,4}^{inc} \end{bmatrix} - \begin{bmatrix} \dfrac{S_1(\psi_1)}{a_3} \dfrac{r_o e^{jk(r_o - r_1)}}{r_1} \\ \dfrac{S_2(\psi_2)}{a_4} \dfrac{r_o e^{jk(r_o - r_2)}}{r_2} \end{bmatrix}. \tag{44}$$

Tubes 3 and 4 both provide the field coupling to the transmission line (Tube 1) and consequently, they will contain the field coupling terns F again. The appropriate equations for the reflected and scattered waves on these tubes are similar to those of Eq.(28), but without the primary source terms, and are given by

$$\begin{bmatrix} E_{3,4}^{ref} \\ E_{3,5}^{ref} \end{bmatrix} = \begin{bmatrix} 0 & \dfrac{r_L e^{jkr_L}}{a_4} \\ \dfrac{r_L e^{jkr_L}}{a_5} & 0 \end{bmatrix} \begin{bmatrix} E_{3,4}^{inc} \\ E_{3,5}^{inc} \end{bmatrix} - \frac{jk}{2\pi a_5} \frac{Z_o}{Z_c} \begin{bmatrix} 0 & 0 \\ F_1(\psi_L) & F_2(\psi_L) \end{bmatrix} \begin{bmatrix} V_{1,1}^{inc} \\ V_{1,2}^{inc} \end{bmatrix}. \tag{45}$$

for Tube 3, and

$$\begin{bmatrix} E_{4,5}^{ref} \\ E_{4,6}^{ref} \end{bmatrix} = \begin{bmatrix} 0 & \dfrac{r_4 e^{jkr_4}}{a_5} \\ \dfrac{r_4 e^{jkr_4}}{a_6} & 0 \end{bmatrix} \begin{bmatrix} E_{4,5}^{inc} \\ E_{4,6}^{inc} \end{bmatrix} - \frac{jk}{2\pi a_5} \frac{Z_o}{Z_c} \begin{bmatrix} F_1(\psi_4) & F_2(\psi_4) \\ 0 & 0 \end{bmatrix} \begin{bmatrix} V_{1,1}^{inc} \\ V_{1,2}^{inc} \end{bmatrix} \tag{46}$$

for Tube 4. Finally, the corresponding field propagation relationships for Tube 5 are

$$\begin{bmatrix} E_{5,4}^{ref} \\ E_{5,6}^{ref} \end{bmatrix} = \begin{bmatrix} 0 & \dfrac{r_3 e^{jkr_3}}{a_4} \\ \dfrac{r_3 e^{jkr_3}}{a_6} & 0 \end{bmatrix} \begin{bmatrix} E_{5,4}^{inc} \\ E_{5,6}^{inc} \end{bmatrix} \tag{47}$$

Equations 42 – 47 can be collected into a 10x10 propagation matrix equation for the reflected voltages and fields at the nodes, as shown in Eq.(48). This equation as the counterpart of Eq(30b) for the simple network of Figure 12.

$$
\begin{bmatrix} V_{1,1}^{ref} \\ V_{1,2}^{ref} \\ a_3 E_{2,3}^{ref} \\ a_4 E_{2,4}^{ref} \\ a_4 E_{3,4}^{ref} \\ a_5 E_{3,5}^{ref} \\ a_5 E_{4,5}^{ref} \\ a_6 E_{4,6}^{ref} \\ a_4 E_{5,4}^{ref} \\ a_6 E_{5,6}^{ref} \end{bmatrix}
=
\begin{bmatrix}
0 & e^{\gamma L} & 0 & 0 & 0 & -\frac{F_1(\psi_L)}{a_5} & -\frac{F_1(\psi_4)}{a_5} & 0 & 0 & 0 \\
e^{\gamma L} & 0 & 0 & 0 & 0 & -\frac{F_2(\psi_L)}{a_5} & -\frac{F_1(\psi_4)}{a_5} & 0 & 0 & 0 \\
0 & 0 & 0 & \frac{r_o}{a_4} e^{jkr_o} & 0 & 0 & 0 & 0 & 0 & 0 \\
0 & 0 & \frac{r_o}{a_3} r_o e^{jkr_o} & 0 & 0 & 0 & 0 & 0 & 0 & 0 \\
0 & 0 & 0 & 0 & 0 & \frac{r_L}{a_5} e^{jkr_L} & 0 & 0 & 0 & 0 \\
-\frac{jk}{2\pi}\frac{Z_o}{Z_c} F_1(\psi_L) & -\frac{jk}{2\pi}\frac{Z_o}{Z_c} F_2(\psi_L) & 0 & 0 & \frac{r_L}{a_4} e^{jkr_L} & 0 & 0 & 0 & 0 & 0 \\
-\frac{jk}{2\pi}\frac{Z_o}{Z_c} F_1(\psi_4) & -\frac{jk}{2\pi}\frac{Z_o}{Z_c} F_2(\psi_4) & 0 & 0 & 0 & 0 & 0 & \frac{r_4}{a_6} e^{jkr_4} & 0 & 0 \\
0 & 0 & 0 & 0 & 0 & 0 & \frac{r_4}{a_5} e^{jkr_4} & 0 & 0 & 0 \\
0 & 0 & 0 & 0 & 0 & 0 & 0 & 0 & 0 & \frac{r_3}{a_6} e^{jkr_3} \\
0 & 0 & 0 & 0 & 0 & 0 & 0 & 0 & \frac{r_3}{a_4} e^{jkr_3} & 0
\end{bmatrix}
\begin{bmatrix} V_{1,1}^{inc} \\ V_{1,2}^{inc} \\ a_3 E_{2,3}^{inc} \\ a_4 E_{2,4}^{inc} \\ a_4 E_{3,4}^{inc} \\ a_5 E_{3,5}^{inc} \\ a_5 E_{4,5}^{inc} \\ a_6 E_{4,6}^{inc} \\ a_4 E_{5,4}^{inc} \\ a_6 E_{5,6}^{inc} \end{bmatrix}
=
\begin{bmatrix} 0 \\ 0 \\ -S_1(\psi_1)\frac{r_o e^{jk(r_o - r_1)}}{r_1} \\ -S_2(\psi_2)\frac{r_o e^{jk(r_o - r_2)}}{r_2} \\ 0 \\ 0 \\ 0 \\ 0 \\ 0 \\ 0 \end{bmatrix}
\qquad (48)
$$

In addition to the propagation relationship of Eq.(48), we can also develop a 10x10 matrix relationship arising from the scattering of waves at the junctions – just as done in Eq.(34b) for the simple problem. In developing this expression, however, we will use a slightly different notation from that used in Eq.(34b). In the following, we let the *superscript* of the reflection coefficient denote the *node* at which the reflection is taking place, and the *subscripts* indicate the various refection coefficient at the node. For example, at Node 1, there is only a simple transmission line voltage reflection coefficient, and it is denoted by ρ_1^1. For this node, the scattering relationship is

$$V_{1,1}^{ref} = \rho_1^1 V_{1,1}^{inc} \tag{49}$$

and the reflection coefficient same as that given in Eq.(9). Similarly, the reflection coefficient on the transmission line at node 2 is given as

$$V_{1,2}^{ref} = \rho_1^2 V_{1,2}^{inc} \tag{50}$$

Node 3 is also a single branch node, but here the E-fields are the important parameters. The scattering relationship is given as

$$E_{2,3}^{ref} = \rho_1^3 E_{2,3}^{inc} \tag{51a}$$

or multiplying by the length parameter a3 to put the field variable into the units of volts, we have

$$a_3 E_{2,3}^{ref} = \rho_1^3 a_3 E_{2,3}^{inc} \tag{51b}$$

The reflection at Node 4 is different, however, because there are three tubes (2,4 and 5) connecting to the aperture. Thus, we require a 3x3 scattering matrix of the form

$$\begin{bmatrix} a_4 E_{2,4}^{ref} \\ a_4 E_{3,4}^{ref} \\ a_4 E_{5,4}^{ref} \end{bmatrix} = \begin{bmatrix} \rho_{1,1}^4 & \rho_{1,2}^4 & \rho_{1,3}^4 \\ \rho_{2,1}^4 & \rho_{2,2}^4 & \rho_{2,3}^4 \\ \rho_{3,1}^4 & \rho_{3,2}^4 & \rho_{3,3}^4 \end{bmatrix} \begin{bmatrix} a_4 E_{2,4}^{inc} \\ a_4 E_{3,4}^{inc} \\ a_4 E_{5,4}^{inc} \end{bmatrix}. \tag{52}$$

Details of this scattering matrix will depend on the aperture size and shape, and also depends on the various angles of incidence and reflection from the aperture. Explicit expressions for these terms remain to be developed for simple apertures, and will be the subject of a future investigation.

Node 5 is the "field coupling node" and as in the simple example case it involves reflections of the fields at this node *with the transmission line removed.* Since there are two tubes (3 and 4) attached here, we expect a 2x2 matrix of the form

$$
\begin{bmatrix} a_5 E_{3,5}^{ref} \\ a_5 E_{4,5}^{ref} \end{bmatrix} = \begin{bmatrix} \rho_{1,1}^5 & \rho_{1,2}^5 \\ \rho_{2,1}^5 & \rho_{2,2}^5 \end{bmatrix} \begin{bmatrix} a_5 E_{3,5}^{inc} \\ a_5 E_{4,5}^{inc} \end{bmatrix}. \tag{53}
$$

Finally, node 6 is a 2-tube connection at the distant scattering body and the pertinent expression for the scattering coefficients is

$$
\begin{bmatrix} a_6 E_{4,6}^{ref} \\ a_6 E_{5,6}^{ref} \end{bmatrix} = \begin{bmatrix} \rho_{1,1}^6 & \rho_{1,2}^6 \\ \rho_{2,1}^6 & \rho_{2,2}^6 \end{bmatrix} \begin{bmatrix} a_6 E_{4,6}^{inc} \\ a_6 E_{5,6}^{inc} \end{bmatrix}. \tag{54}
$$

The individual node scattering relationships in Eqs.(49) – (54) can be put into a large 10x10 matrix equation. In doing this, however, we must re-order the matrix entries so that the ordering of the incident and reflected voltage/field vectors correspond to that in the propagation matrix equation in Eq.(48). This results in the following system scattering matrix:

$$
\begin{bmatrix} V_{1,1}^{ref} \\ V_{1,2}^{ref} \\ a_3 E_{2,3}^{ref} \\ a_4 E_{2,4}^{ref} \\ a_4 E_{3,4}^{ref} \\ a_5 E_{3,5}^{ref} \\ a_5 E_{4,5}^{ref} \\ a_6 E_{4,6}^{ref} \\ a_4 E_{5,4}^{ref} \\ a_6 E_{5,6}^{ref} \end{bmatrix} = \begin{bmatrix}
\rho_1^1 & 0 & 0 & 0 & 0 & 0 & 0 & 0 & 0 & 0 \\
0 & \rho_1^2 & 0 & 0 & 0 & 0 & 0 & 0 & 0 & 0 \\
0 & 0 & \rho_1^3 & 0 & 0 & 0 & 0 & 0 & 0 & 0 \\
0 & 0 & 0 & \rho_{1,1}^4 & \rho_{1,2}^4 & 0 & 0 & 0 & \rho_{1,3}^4 & 0 \\
0 & 0 & 0 & \rho_{2,1}^4 & \rho_{2,2}^4 & 0 & 0 & 0 & \rho_{2,3}^4 & 0 \\
0 & 0 & 0 & 0 & 0 & \rho_{1,1}^5 & \rho_{1,2}^5 & 0 & 0 & 0 \\
0 & 0 & 0 & 0 & 0 & \rho_{2,1}^5 & \rho_{2,2}^5 & 0 & 0 & 0 \\
0 & 0 & 0 & 0 & 0 & 0 & 0 & \rho_{1,1}^6 & 0 & \rho_{1,2}^6 \\
0 & 0 & 0 & \rho_{3,1}^4 & \rho_{3,2}^4 & 0 & 0 & 0 & \rho_{3,3}^4 & 0 \\
0 & 0 & 0 & 0 & 0 & 0 & 0 & \rho_{2,1}^6 & 0 & \rho_{2,2}^6
\end{bmatrix} \begin{bmatrix} V_{1,1}^{inc} \\ V_{1,2}^{inc} \\ a_3 E_{2,3}^{inc} \\ a_4 E_{2,4}^{inc} \\ a_4 E_{3,4}^{inc} \\ a_5 E_{3,5}^{inc} \\ a_5 E_{4,5}^{inc} \\ a_6 E_{4,6}^{inc} \\ a_4 E_{5,4}^{inc} \\ a_6 E_{5,6}^{inc} \end{bmatrix} \tag{55}
$$

Substituting this equation into Eq(48) and solving for the incident voltage vector gives the first form of the BLT equation for the incident response components, as reported in Eq.(56). Adding Eqs.(55) and (56) yields the total responses at the nodes, as given by Eq.(57).

$$
\begin{bmatrix} V_{1,1}^{ref} \\ V_{1,2}^{ref} \\ a_3E_{2,3}^{ref} \\ a_4E_{2,4}^{ref} \\ a_4E_{3,4}^{ref} \\ a_5E_{3,5}^{ref} \\ a_5E_{4,5}^{ref} \\ a_6E_{4,6}^{ref} \\ a_4E_{5,4}^{ref} \\ a_6E_{5,6}^{ref} \end{bmatrix}
=
\begin{bmatrix}
-\rho_1^1 & e^{\gamma L} & 0 & 0 & 0 & -\frac{F_1(\psi_L)}{a_5} & -\frac{F_1(\psi_4)}{a_5} & 0 & 0 & 0 \\
e^{\gamma L} & -\rho_1^2 & 0 & 0 & 0 & -\frac{F_2(\psi_L)}{a_5} & -\frac{F_1(\psi_4)}{a_5} & 0 & 0 & 0 \\
0 & 0 & -\rho_1^3 & \frac{r_o}{a_4}e^{jkr_o} & 0 & 0 & 0 & 0 & 0 & 0 \\
0 & 0 & \frac{r_o}{a_3}r_o e^{jkr_o} & -\rho_{1,1}^4 & -\rho_{1,2}^4 & 0 & 0 & 0 & -\rho_{1,3}^4 & 0 \\
0 & 0 & 0 & -\rho_{2,1}^4 & -\rho_{2,2}^4 & \frac{r_L}{a_5}e^{jkr_L} & 0 & 0 & -\rho_{2,3}^4 & 0 \\
-\frac{jk}{2\pi}\frac{Z_o}{Z_c}F_1(\psi_L) & -\frac{jk}{2\pi}\frac{Z_o}{Z_c}F_2(\psi_L) & 0 & 0 & \frac{r_L}{a_4}e^{jkr_L} & -\rho_{1,1}^5 & -\rho_{1,2}^5 & 0 & 0 & 0 \\
-\frac{jk}{2\pi}\frac{Z_o}{Z_c}F_1(\psi_4) & -\frac{jk}{2\pi}\frac{Z_o}{Z_c}F_2(\psi_4) & 0 & 0 & 0 & -\rho_{2,1}^5 & -\rho_{2,2}^5 & \frac{r_4}{a_6}e^{jkr_4} & 0 & 0 \\
0 & 0 & 0 & 0 & 0 & 0 & \frac{r_4}{a_5}e^{jkr_4} & -\rho_{1,1}^6 & 0 & -\rho_{1,2}^6 \\
0 & 0 & 0 & -\rho_{3,1}^4 & -\rho_{3,2}^4 & 0 & 0 & 0 & -\rho_{3,3}^4 & \frac{r_3}{a_6}e^{jkr_3} \\
0 & 0 & 0 & 0 & 0 & 0 & 0 & -\rho_{2,1}^6 & \frac{r_3}{a_4}e^{jkr_3} & -\rho_{2,2}^6
\end{bmatrix}^{-1}
=
\begin{bmatrix} 0 \\ 0 \\ S_1(\psi_1)\frac{r_o e^{jk(r_o-r_1)}}{r_1} \\ S_2(\psi_2)\frac{r_o e^{jk(r_o-r_2)}}{r_2} \\ 0 \\ 0 \\ 0 \\ 0 \\ 0 \\ 0 \end{bmatrix}
\qquad (56)
$$

$$
\begin{bmatrix} V_{1,1} \\ V_{1,2} \\ a_3E_{2,3} \\ a_4E_{2,4} \\ a_4E_{3,4} \\ a_5E_{3,5} \\ a_5E_{4,5} \\ a_6E_{4,6} \\ a_4E_{5,4} \\ a_6E_{5,6} \end{bmatrix}
=
\begin{bmatrix}
1+\rho_1^1 & 0 & 0 & 0 & 0 & 0 & 0 & 0 & 0 & 0 \\
0 & 1+\rho_1^2 & 0 & 0 & 0 & 0 & 0 & 0 & 0 & 0 \\
0 & 0 & 1+\rho_1^3 & 0 & 0 & 0 & 0 & 0 & 0 & 0 \\
0 & 0 & 0 & 1+\rho_{1,1}^4 & \rho_{1,2}^4 & 0 & 0 & 0 & \rho_{1,3}^4 & 0 \\
0 & 0 & 0 & \rho_{2,1}^4 & 1+\rho_{2,2}^4 & 0 & 0 & 0 & \rho_{2,3}^4 & 0 \\
0 & 0 & 0 & 0 & 0 & 1+\rho_{1,1}^5 & \rho_{1,2}^5 & 0 & 0 & 0 \\
0 & 0 & 0 & 0 & 0 & \rho_{2,1}^5 & 1+\rho_{2,2}^5 & 0 & 0 & 0 \\
0 & 0 & 0 & 0 & 0 & 0 & 0 & 1+\rho_{1,1}^6 & 0 & \rho_{1,2}^6 \\
0 & 0 & 0 & \rho_{3,1}^4 & \rho_{3,2}^4 & 0 & 0 & 0 & 1+\rho_{3,3}^4 & 0 \\
0 & 0 & 0 & 0 & 0 & 0 & 0 & \rho_{2,1}^6 & 0 & 1+\rho_{2,2}^6
\end{bmatrix}
\times
$$

$$
\begin{bmatrix}
-\rho_1^1 & e^{\gamma L} & 0 & 0 & 0 & -\frac{F_1(\psi_L)}{a_5} & -\frac{F_1(\psi_4)}{a_5} & 0 & 0 & 0 \\
e^{\gamma L} & -\rho_1^2 & 0 & 0 & 0 & -\frac{F_2(\psi_L)}{a_5} & -\frac{F_1(\psi_4)}{a_5} & 0 & 0 & 0 \\
0 & 0 & -\rho_1^3 & \frac{r_o}{a_4}e^{jkr_o} & 0 & 0 & 0 & 0 & 0 & 0 \\
0 & 0 & \frac{r_o}{a_3}r_oe^{jkr_o} & -\rho_{1,1}^4 & -\rho_{1,2}^4 & 0 & 0 & 0 & -\rho_{1,3}^4 & 0 \\
0 & 0 & 0 & -\rho_{2,1}^4 & -\rho_{2,2}^4 & \frac{r_L}{a_5}e^{jkr_L} & 0 & 0 & -\rho_{2,3}^4 & 0 \\
-\frac{jk}{2\pi}\frac{Z_o}{Z_c}F_1(\psi_L) & -\frac{jk}{2\pi}\frac{Z_o}{Z_c}F_2(\psi_L) & 0 & 0 & \frac{r_L}{a_4}e^{jkr_L} & -\rho_{1,1}^5 & -\rho_{1,2}^5 & 0 & 0 & 0 \\
-\frac{jk}{2\pi}\frac{Z_o}{Z_c}F_1(\psi_4) & -\frac{jk}{2\pi}\frac{Z_o}{Z_c}F_2(\psi_4) & 0 & 0 & 0 & -\rho_{2,1}^5 & -\rho_{2,2}^5 & \frac{r_4}{a_6}e^{jkr_4} & 0 & 0 \\
0 & 0 & 0 & 0 & 0 & 0 & \frac{r_4}{a_5}e^{jkr_4} & -\rho_{1,1}^6 & 0 & -\rho_{1,2}^6 \\
0 & 0 & 0 & -\rho_{3,1}^4 & -\rho_{3,2}^4 & 0 & 0 & 0 & -\rho_{3,3}^4 & \frac{r_3}{a_6}e^{jkr_3} \\
0 & 0 & 0 & 0 & 0 & 0 & 0 & -\rho_{2,1}^6 & \frac{r_3}{a_4}e^{jkr_3} & -\rho_{2,2}^6
\end{bmatrix}^{-1}
\times
\begin{bmatrix} 0 \\ 0 \\ S_1(\psi_1)\frac{r_oe^{jk(r_o-r_1)}}{r_1} \\ S_2(\psi_2)\frac{r_oe^{jk(r_o-r_2)}}{r_2} \\ 0 \\ 0 \\ 0 \\ 0 \\ 0 \\ 0 \end{bmatrix}
\quad (57)
$$

5. Summary

This paper has outlined an analysis methodology for treating EM scattering and aperture penetration problems with the formalism of the BLT equation. In addition to the usual transmission line paths on which voltage and current waves propagate with little attenuation, in the extended problem has EM "signal paths" that have a 1/r attenuation, and which are able to couple to transmission line structures along the length of the line, not just at the end nodes.

To analyze this field coupling phenomenon, we introduce the concept of a "field coupling node", which takes into account the incident EM field coupling to the transmission line. Moreover, by reciprocity, this node also provides effects of EM field radiation by the transmission line back to the source or other scatterers in the problem space.

To illustrate this methodology, two examples have been given: a simple radiating source coupling to an isolated transmission line, and a source near an aperture in a shield, coupling to a line, with several scattering objects nearby. In both of these cases, only the analysis methodology has been outlines; numerical calculations and verification of this analysis have yet to be done, and will be the subject of a subsequent note.

6. References

1. Workshop on "Electromagnetic Terrorism and Adverse Effects of High Power Electromagnetic (HPE) Environments", *Proceedings of the 13th International Zurich Symposium and Technical Exhibition on Electromagnetic Compatibility*, Feb. 1999.

2. *EMP Interaction: Principles, Techniques and Reference Data*, K.S.H. Lee, editor, AFWL-TR-80-402, 1981. Also reprinted by Taylor and Francis, New York, 1989.

3. Baum, C. E., "How to Think About EMP Interaction", *Proceedings of the 1974 Spring FULMEN Meeting*, Kirtland AFB, April 1974.

4. Tesche, F. M., et. al., "Internal Interaction Analysis: Topological Concepts and Needed Model Improvements", *Interaction Note Series*, IN-248, October 1975.

5. Tesche, F. M., "Topological Concepts for Internal EMP Interaction," *IEEE Trans. AP*, Vol. AP-26, No. 1, January 1978.

6. Baum, C. E., "Electromagnetic Topology for the Analysis and Design of Complex Electromagnetic Systems", **Fast Electrical and Optical Measurements**, Vol. I, eds. I.E. Thompson and L.H. Luessen, Martinus Nijhoff, Dordrecht, 1986.

7. Tesche, F.M., "Introduction to Concepts of Electromagnetic Topology as Applied to EMP Interaction With Systems", NATO/AGARD Lecture Series Publication 144, *Interaction Between EMP, Lightning and Static Electricity with Aircraft and Missile Avionics Systems*, May 1986.

8. Tesche, F. M., et. al., **EMC Analysis Methods and Computational Models**, John Wiley and Sons, New York, 1997.

9. Baum, C.E., Liu, T.K, & Tesche, F.M., "On the Analysis of General Multiconductor Transmission Line Networks", *Interaction Note 350*, Kirtland AFB, NM, 1978.

10. Baum, C.E., "Generalization of the BLT Equation, *Proceedings of the 13th Zurich EMC Symposium*, Feb. 1999, pp. 131-136. Also *Interaction Note 511*, April 1995.

11. Baum, C. E., "Extension of the BLT Equation into Time Domain", *Interaction Note 553*, 24 March 1999.

12. Tesche, F. M., and T.K. Liu, "User Manual and Code Description for QV7TA: a General Multiconductor Transmission Line Analysis Code", LuTech, Inc. report, August 1978.

13. Parmantier, J-P, "First Realistic Simulation of Effects of EM Coupling in Commercial Aircraft Wiring", *IEE Computing & Control Engineering Journal*, April 1998.

14. Tesche, F. M., "Plane Wave Coupling to Cables", Chapter 4 in Part II of **Handbook of Electromagnetic Compatibility**, R. Perez, ed., Academic Press, 1995.

15. Baum, C. E., "Including Apertures and Cavities in the BLT Formalism", Interaction Notes, Note 581, 27 January 2003.

Appendix A

Field Excitation of a Transmission Line using the BLT Equation

In this appendix we wish to derive the BLT equations for the load voltages and currents for the case of distributed field excitation of the transmission line, as portrayed in Figure A1. As discussed in [A1], this excitation can be represented by the tangential incident E-field along the line and at the end conductors of the terminating impedances. Generally, the distributed voltage sources will induce both antenna mode and transmission line mode responses, but as previously mentioned, we will consider only the transmission line responses in this discussion.

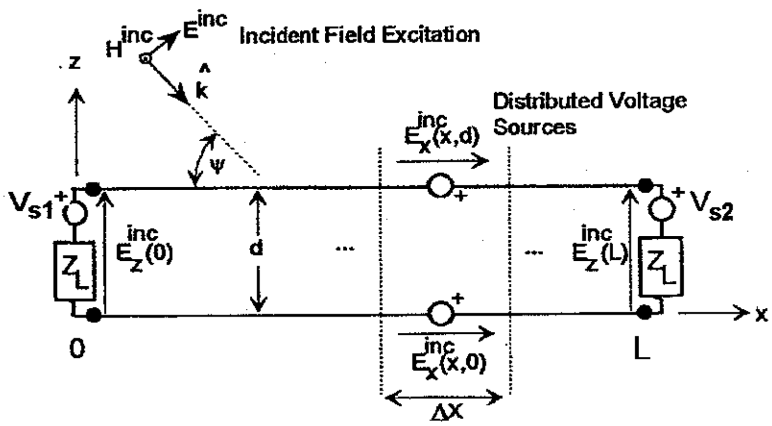

Figure A1.Field excitation of a two-wire transmission line, showing the voltage excitation sources needed in the BLT equation.

The transmission line excitation along the length of the line can be represented by a *distributed* voltage source, $V_s'(x)$ which is given by the difference of the x-components of the incident E-field along the line. This is expressed as

$$V_s'(x) = E_x^{inc}(x,d) - E_x^{inc}(x,0) . \qquad \text{(A1)}$$

In addition, there are two lumped voltage sources at either ends of the line, V_{s1} and V_{s2}, which take into account the interaction of the incident E-field with the vertical conductors in the loads at the ends of the line. These are given in terms of the z-components of the incident E-field, evaluated at $z = 0$, and are expressed as

$$V_{s1} \approx E_z^{inc}(0,0)d \quad and \quad V_{s1} \approx E_z^{inc}(L,0)d . \qquad \text{(A2)}$$

The load responses given by the BLT equations (14) or (16) in the main body of this report can be thought of as Green's functions for computing the responses due to a distributed field excitation. Setting the current excitation term to zero in Eq.(14), the following Green's function for the load voltages due to a lumped voltage source at location x can be defined:

$$\begin{bmatrix} G_1(x) \\ G_2(x) \end{bmatrix} = \begin{bmatrix} 1+\rho_1 & 0 \\ 0 & 1+\rho_2 \end{bmatrix} \cdot \begin{bmatrix} -\rho_1 & e^{\gamma L} \\ e^{\gamma L} & -\rho_2 \end{bmatrix}^{-1} \cdot \begin{bmatrix} \frac{1}{2}V_s(x)e^{\gamma x} \\ -\frac{1}{2}V_s(x)e^{\gamma(L-x)} \end{bmatrix}. \tag{A3}$$

Here $G_1(x)$ denotes the Green's function for the load voltage response at node 1 and $G_2(x)$ is the Green's function for the voltage at node 2. Similar Green's functions for the load currents can be defined using Eq.(16).

It is clear that by inserting in the voltage source distributions given by Eqs.(A1) and (A2) into Eq.(A3) and integrating over the transmission line, the only modification to the BLT equation is a change of the source terms. In this manner, the BLT voltage equation for distributed source excitation becomes

$$\begin{bmatrix} V_1 \\ V_2 \end{bmatrix} = \begin{bmatrix} 1+\rho_1 & 0 \\ 0 & 1+\rho_2 \end{bmatrix} \cdot \begin{bmatrix} -\rho_1 & e^{\gamma L} \\ e^{\gamma L} & -\rho_2 \end{bmatrix}^{-1} \cdot \begin{bmatrix} S_1 \\ S_2 \end{bmatrix}, \tag{A4}$$

where the source vector is now given as

$$\begin{bmatrix} S_1 \\ S_2 \end{bmatrix} = \frac{1}{2} \begin{bmatrix} \int_0^L \left(E_x^{inc}(x,d) - E_x^{inc}(x,0)\right) e^{\gamma x_s} dx + E_z^{inc}(0,0)d - E_z^{inc}(L,0)d\, e^{\gamma L} \\ -\int_0^L \left(E_x^{inc}(x,d) - E_x^{inc}(x,0)\right) e^{\gamma(L-x_s)} dx - E_z^{inc}(0,0)d\; e^{\gamma L} + E_z^{inc}(L,0)d \end{bmatrix}. \tag{A5}$$

Note that in this equation, the first term in the source vector is the integral term accounting for the effects of the distributed field excitation of the line, and the second and third lumped terms account for the excitation of the end conductors of the line.

For the special case of a vertically polarized plane wave of amplitude E^{inc} propagating in the $x-z$ plane with an incidence angle ψ (as shown in Figure A1), the x and z components of the incident E-field can be written as

$$E_x^{inc}(x,z) = E^{inc} \sin\psi\, e^{-jkx\cos\psi} e^{jkz\sin\psi}. \tag{A6a}$$

$$E_z^{inc}(x,z) = E^{inc} \cos\psi\, e^{-jkx\cos\psi} e^{jkz\sin\psi} \tag{A6b}$$

Assuming that the transmission line propagation constant is the same as that of free space (e.g., $\gamma = jk$), inserting the above expressions for the incident E-fields into Eq.(A5), performing the indicated integrations and then combining terms provides the following expression for the source vector for plane wave excitation of the line:

$$\begin{bmatrix} S_1 \\ S_2 \end{bmatrix} = \frac{E^{inc} d}{2} \begin{bmatrix} \left(e^{jkL(1-\cos\psi)} - 1\right) \\ e^{jkL}\left(e^{-jkL(1+\cos\psi)} - 1\right) \end{bmatrix} . \qquad \text{(A7)}$$
$$\equiv E^{inc} \begin{bmatrix} F_1(\psi) \\ F_2(\psi) \end{bmatrix}$$

This last equation serves to define the field coupling functions F_1 and F_2, which define how strongly the traveling waves are excited by the incident field. Note that ref.[1] presents the more general expression for this source vector for the case of an arbitrarily incident and polarized EM field acting on the line and for the case of the transmission line propagation constant γ differing from the free space propagation constant.

As in the case of a single lumped excitation source on the line, the S_1 source term in Eq.(A7) can be attributed to the positive traveling wave on the line, as excited by the incident field, and the S_2 term is due to the excitation of the negative traveling wave.

References

A1. Tesche, F. M., et. al., **EMC Analysis Methods and Computational Models**, John Wiley and Sons, New York, 1997.

Appendix B

Radiation Fields Produced by Traveling Wave Components on a Transmission Line

One of the elements needed in the generalization of the BLT equation to include field propagation effects is the radiation produced by traveling waves on a transmission line. As noted in [B1], this can be determined using the concepts of electromagnetic reciprocity. Alternatively, it is possible to simply integrate over the current distribution on the line, which arises from the traveling wave currents. This latter approach is considered in this appendix.

Figure B1 shows a transmission line of length L with a positive traveling voltage wave $V^+(x)$. Not shown in this diagram is a corresponding negative traveling wave. Both of these waves are excited in some manner by some sort of an excitation function, and the behavior of these waves is determined by the termination impedances and the excitation function. At this stage, we are not interested in the complete solution of the voltage or current on the line (as this ultimately arises from a solution of the BLT equation), but we are seeking to determine the radiated field contributions from each of these traveling waves – expressed in terms of the incident voltage waves at each end of the line.

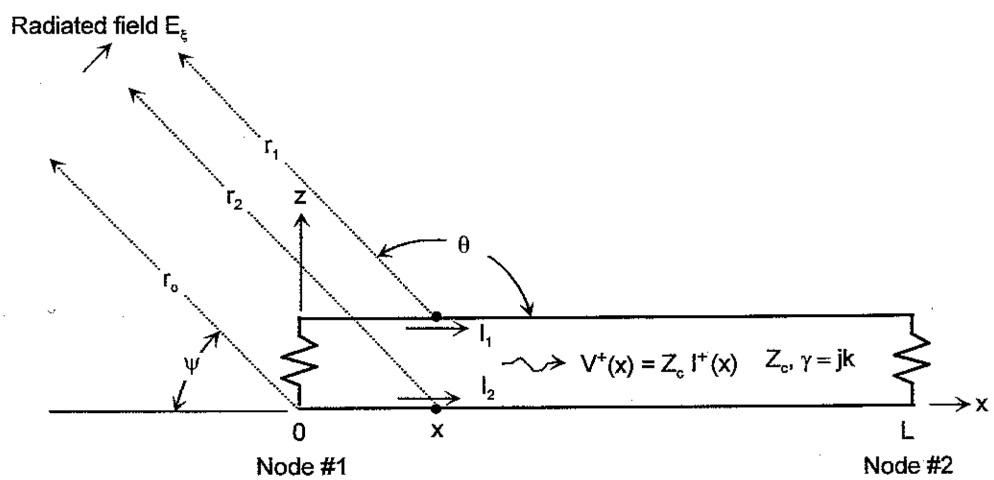

Figure B1. Illustration of a positive traveling wave on a transmission line, with the production of a radiated field E_ξ.

The radiated E-field is assumed to be in the ψ direction at a distance r_o from the origin of the coordinate system, as shown in the figure. We assume that r_o is sufficiently far from the line so that the radiated field is a plane wave, with primary component E_ξ.

For the positive traveling voltage wave $V^+(x)$, the corresponding current traveling wave is given as $I^+(x) = V^+(x)/Z_c$, where Z_c is the characteristic impedance of the transmission line.

For this traveling current wave, there are individual traveling wave currents on each conductor of the line given by I_1 and I_2, as shown in Figure B1, with the constraint that $I_2 = -I_1$.

To determine the E-field radiated by the traveling wave currents on this line, it is necessary to recall the fundamental radiation formula for the field produced by an infinitesimal current element *Idl*, as shown in Figure B2. In the far-zone, the radiated E-field is given as [B1]

$$E_\theta = \frac{j\omega\mu_o}{4\pi r_o}\sin\theta\; Idl\, e^{-jkr_o} \tag{B1}$$

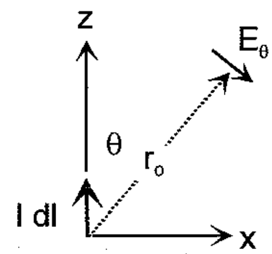

Figure B2. Radiation field geometry for a point current element, *I dl*.

Noting that E_θ is in the opposite direction than the field component E_ξ in Figure B1, and that $\sin\theta = \sin\psi$, the differential radiated E-field component due to the pair of currents at location x on the line may be expressed as

$$dE_\xi = -\frac{j\omega\mu_o}{4\pi}\sin\psi\left(I_1(x)\frac{e^{-jkr_1}}{r_1} + I_2(x)\frac{e^{-jkr_2}}{r_2}\right) \tag{B2}$$

Using the fact that the traveling wave currents can be expressed in terms of the incident traveling voltage wave at node 2 (at $x = L$) as

$$I_1(x) = -I_2(x) = \frac{V_2^{inc}}{Z_c}e^{-\gamma(x-L)}, \tag{B3}$$

together with the far-field approximations

$$\frac{1}{r_1} \approx \frac{1}{r_2} \approx \frac{1}{r_o} \tag{B4a}$$

$$e^{-jkr_1} = e^{-jk(r_o + x\cos\psi - d\sin\psi)} \tag{B4b}$$

$$e^{-jkr_2} = e^{-jk(r_o + x\cos\psi)} \tag{B4c}$$

the differential field becomes

$$dE_\xi = -\frac{j\omega\mu_o}{4\pi r_o}\sin\psi \frac{V_2^{inc}}{Z_c} e^{-\gamma(x-L)} e^{-jk(r_o + x\cos\psi)}\left(e^{jkd\sin\psi} - 1\right). \qquad \text{(B5)}$$

Noting that $\left(e^{jkd\sin\psi} - 1\right) \approx jkd\sin\psi$ and assuming again that $\gamma = jk$, Eq.(B5) can be put into the following form:

$$dE_\xi = \frac{k^2 d}{4\pi}\frac{Z_o}{Z_c}\frac{e^{-jkr_o}}{r_o}\sin^2\psi\, V_2^{inc} e^{jkL} e^{-jk(1+\cos\psi)x}. \qquad \text{(B6)}$$

To obtain the total contribution to the radiated E-field from the traveling wave currents, Eq.(B6) must be integrated over the length of the line. This is expressed as

$$\begin{aligned} E_\xi^1 &= \int_0^L E_\xi(x)dx = \frac{k^2 d}{4\pi}\frac{Z_o}{Z_c}\frac{e^{-jkr_o}}{r_o}\sin^2\psi\; V_2^{inc} e^{jkL}\int_0^L e^{-jk(1+\cos\psi)x}dx \\ &= \frac{k^2 d}{4\pi}\frac{Z_o}{Z_c}\frac{e^{-jkr_o}}{r_o}\sin^2\psi\; V_2^{inc} e^{jkL}\frac{\left(e^{-jk(1+\cos\psi)L} - 1\right)}{-jk(1+\cos\psi)} \\ &= \frac{jkd}{4\pi}\frac{Z_o}{Z_c}\frac{e^{-jkr_o}}{r_o} V_2^{inc} e^{jkL}\frac{\sin^2\psi}{(1+\cos\psi)}\left(e^{-jk(1+\cos\psi)L} - 1\right) \end{aligned} \qquad \text{(B7)}$$

The radiated field in Eq.(B7) is not the complete field from the positive traveling wave, however, because the contributions of the traveling wave components in the end loads have not been included. As shown in Figure B3 there is a current I_1 flowing in the end of the line at $x = 0$, and a current I_2 at the end at $x = L$. These currents may both be expressed in terms of the incident voltage wave at node 2 as

$$I_1 = \frac{V_2^{inc}}{Z_c} e^{jkL} \qquad \text{(B8a)}$$

and

$$I_2 = -\frac{V_2^{inc}}{Z_c}. \qquad \text{(B8b)}$$

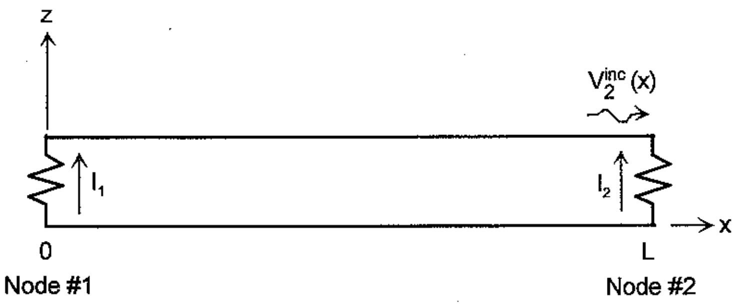

Figure B3. The traveling wave currents at the vertical ends of the transmission line.

Using the expression (B1) again, the E-field contribution from these end currents can be written as

$$\begin{aligned} E_\xi^2 &= -\frac{j\omega\mu_o}{4\pi r_o}\cos\psi\, e^{-jkr_o}\left(I_1 d + I_2 d e^{-jkL\cos\psi}\right) \\ &= -\frac{j\omega\mu_o}{4\pi r_o}\cos\psi\, e^{-jkr_o}\frac{V_2^{inc}}{Z_c}e^{jkL}\left(1-e^{-jk(1+\cos\psi)L}\right). \\ &= \frac{jkd}{4\pi}\frac{Z_o}{Z_c}\frac{e^{-jkr_o}}{r_o}V_2^{inc}e^{jkL}\cos\psi\left(e^{-jk(1+\cos\psi)L}-1\right) \end{aligned} \quad \text{(B9)}$$

Combining Eqs.(B7) and (B9) provides the total radiated field from the positive traveling wave component as

$$\begin{aligned} E_\xi^+ = E_\xi^1 + E_\xi^2 &= \frac{jkd}{4\pi}\frac{Z_o}{Z_c}\frac{e^{-jkr_o}}{r_o}V_2^{inc}e^{jkL}\left(e^{-jk(1+\cos\psi)L}-1\right)\left[\frac{\sin^2\psi}{(1+\cos\psi)}+\cos\psi\right] \\ &= \frac{jkd}{4\pi}\frac{Z_o}{Z_c}\frac{e^{-jkr_o}}{r_o}V_2^{inc}e^{jkL}\left(e^{-jk(1+\cos\psi)L}-1\right) \end{aligned} \quad \text{.(B10)}$$

Using the definition of the *backward* wave field coupling function F_2, as defined by Eq.(A7) in Appendix A, the radiated field for the *positive* traveling wave on the line given in Eq.(B10) can be written as

$$E_\xi^+ = \frac{jk}{2\pi}\frac{Z_o}{Z_c}\frac{e^{-jkr_o}}{r_o}F_2(\psi)V_2^{inc}, \quad \text{(B10)}$$

which is essentially a statement of reciprocity between the reception and transmission properties of the transmission line.

In a similar manner to the development above, the E-field produced by the traveling wave components on the line and in the end loads can be computed. In this instance, the expression will be developed in terms of the incident voltage wave at node 1, V_1^{inc} to ultimately be compatible with the requirements of the BLT equation. Upon carrying out the required integration and simplification of results, the E-field from this negative traveling wave (including the end current effects) is

$$\begin{aligned} E_\xi^- = E_\xi^1 + E_\xi^2 &= \frac{jkd}{4\pi}\frac{Z_o}{Z_c}\frac{e^{-jkr_o}}{r_o} V_1^{inc}\left(e^{jk(1-\cos\psi)L} - 1\right)\left[\frac{\sin^2\psi}{(1-\cos\psi)} - \cos\psi\right] \\ &= \frac{jkd}{4\pi}\frac{Z_o}{Z_c}\frac{e^{-jkr_o}}{r_o} V_1^{inc}\left(e^{jk(1-\cos\psi)L} - 1\right) \\ &= \frac{jk}{2\pi}\frac{Z_o}{Z_c}\frac{e^{-jkr_o}}{r_o} V_1^{inc} F_1(\psi) \end{aligned} \qquad \text{(B11)}$$

where $F_1(\psi)$ is the field coupling function for positive traveling waves on the receiving transmission line, given by Eq.(A7) of Appendix A.

By combining Eqs.(B10) and (B11), the total E-field radiated by the two traveling waves on the line can be determined:

$$E_\xi = E_\xi^+ + E_\xi^- = \frac{jk}{2\pi}\frac{Z_o}{Z_c}\frac{e^{-jkr_o}}{r_o}\left(V_1^{inc} F_1(\psi) + V_2^{inc} F_2(\psi)\right). \qquad \text{(B12)}$$

References

B1. Tesche, F. M., et. al., **EMC Analysis Methods and Computational Models**, John Wiley and Sons, New York, 1997.